

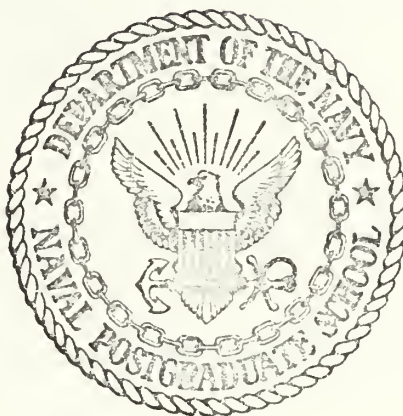
WAVE-RELATED VELOCITY FLUCTUATIONS
OVER OCEAN WAVES AS
MEASURED FROM FLIP DURING BOMEX

David Robert Aurand

Library
Naval Postgraduate School
Monterey, California 93940

NAVAL POSTGRADUATE SCHOOL

Monterey, California



THESIS

WAVE-RELATED VELOCITY FLUCTUATIONS
OVER OCEAN WAVES AS
MEASURED FROM FLIP DURING BOMEX

by

David Robert Aurand

Thesis Advisor:

K. L. Davidson

March 1973

U1-5574

Approved for public release; distribution unlimited.

Wave-Related Velocity Fluctuations
over Ocean Waves as
Measured from FLIP during BOMEX

by

David Robert Aurand
Lieutenant, United States Navy
B.S., University of Missouri at
Kansas City, 1965

Submitted in partial fulfillment of the
requirements for the degree of

MASTER OF SCIENCE IN METEOROLOGY

from the

ABSTRACT

Wave-related velocity fluctuations over ocean waves and wave heights as measured from FLIP during BOMEX are examined using phase-amplitude results which are based on joint probability density function-conditional mean function (JPDF-CMF) analyses. Results are compared with predictions from various wind-wave coupling models.

Results are examined in detail and consistent departures from theory are noted. An attempt is made to qualitatively determine the effect on specific results of the moving, but relatively stable, sensor platform, FLIP.

It is concluded that the interaction between the wave-induced motion and airflow turbulence had a significant effect on the observed wave-related fluctuations. The effects of FLIP on the results appeared to be minimal on these results.

TABLE OF CONTENTS

I.	INTRODUCTION - - - - -	8
II.	BACKGROUND - - - - -	10
	A. SEA-AIR INTERACTION EXPERIMENT - - - - -	10
	B. THEORETICAL BACKGROUND - - - - -	10
	C. OBSERVATIONAL BACKGROUND - - - - -	12
III.	DATA COLLECTION- - - - -	17
	A. INSTRUMENTATION- - - - -	17
	B. FLOATING INSTRUMENT PLATFORM (FLIP)- - - - -	17
IV.	THE PREPARATION AND ANALYSIS OF DATA - - - - -	20
	A. INITIAL DATA PREPARATION - - - - -	20
	B. BAND PASS FILTERING AND NORMALIZATION- - - - -	21
	C. JPDF-CMF PROCEDURES- - - - -	22
	D. PHASE-AMPLITUDE COMPUTATIONAL PROCEDURES - - - - -	22
V.	PRESENTATION OF RESULTS- - - - -	27
	A. PERIOD 12- - - - -	31
	B. PERIOD 1 - - - - -	43
	C. PERIOD 6 - - - - -	48
	D. PERIOD 14- - - - -	53
VI.	SUMMARY AND CONCLUSIONS- - - - -	59
	APPENDIX A - - - - -	61
	BIBLIOGRAPHY - - - - -	66
	INITIAL DISTRIBUTION LIST- - - - -	68
	FORM DD 1473 - - - - -	69

LIST OF TABLES

I. Summary of Analyzed Periods- - - - -	28
---	----

LIST OF FIGURES

1.	Phase-Amplitude Relations Predicted by Potential Flow Theory for the Two Components of Velocity (u and w) and the Stress uw, with Respect to the Wave - - - - -	13
2.	View of FLIP Showing the Arrangement of Sensors during BOMEX - - - - -	18
3.	Top View of FLIP Showing the Mooring Procedure Employed during BOMEX- - - - -	18
4.	Response Curve of the Band Pass Numerical Inverse Transform Filter - - - - -	21
5.	Two-Dimensional JPDF-CMF Array - - - - -	24
6.	Phase-Amplitude Results Showing the Resolution Achieved by Summing over 30° Segments- - - - -	26
7.	Phase-Amplitude Results Showing the Resolution Achieved by Summing over 45° Segments as Used by Previous Investigators- - - - -	26
8.	Measurements and Wind and Wave Condition - - - - -	29
9.	Phase-Amplitude Results for Period 12a, Subset 1 (8 meter level) - - - - -	35
10.	Phase-Amplitude Results for Period 12a, Subset 2 (8 meter level) - - - - -	36
11.	Phase-Amplitude Results for Period 12a, Subset 3 (8 meter level) - - - - -	37
12.	Phase-Amplitude Results for Period 12a, Subset 4 (8 meter level) - - - - -	38
13.	Phase-Amplitude Results for Period 12b, Subset 1 (3 meter level) - - - - -	39
14.	Phase-Amplitude Results for Period 12b, Subset 2 (3 meter level) - - - - -	40
15.	Phase-Amplitude Results for Period 12b, Subset 3 (3 meter level) - - - - -	41
16.	Phase-Amplitude Results for Period 12b, Subset 4 (3 meter level) - - - - -	42

17.	Phase-Amplitude Results for Period 1, Subset 1 - - - - -	44
18.	Phase-Amplitude Results for Period 1, Subset 2 - - - - -	45
19.	Phase-Amplitude Results for Period 1, Subset 3 - - - - -	46
20.	Phase-Amplitude Results for Period 1, Subset 4 - - - - -	47
21.	Phase-Amplitude Results for Period 6, Subset 1 - - - - -	50
22.	Phase-Amplitude Results for Period 6, Subset 2 - - - - -	51
23.	Phase-Amplitude Results for Period 6, Subset 3 - - - - -	52
24.	Phase-Amplitude Results for Period 14, Subset 1 - - - - -	55
25.	Phase-Amplitude Results for Period 14, Subset 2 - - - - -	56
26.	Phase-Amplitude Results for Period 14, Subset 3 - - - - -	57
27.	Phase-Amplitude Results for Period 14, Subset 4 - - - - -	58
28.	The Fixed Reference Coordinate System Has Its Origin at the Metacenter of the Spar Buoy. For Small Pitch-Roll Displacements the Metacenter is Fixed. - - - - -	62

ACKNOWLEDGEMENTS

The author wishes to express his appreciation to his advisor, Dr. K. L. Davidson, for his support, advice, and assistance throughout this project.

Appreciation is also expressed to Dr. R. T. Williams for his careful review of the manuscript and useful suggestions, to Lieutenant R. J. Stricker for his assistance in data filtering, and to Dr. A. W. Green of the Department of Meteorology and Oceanography, University of Michigan, for his useful description of the motions of the instrument platform.

Numerical calculations were performed at the University of Michigan computer facility and by the W. R. Church Computer Center of the Naval Postgraduate School. The research was made possible by the Office of Naval Research Project Order 3-0016 dated 1 July 1972 with the Naval Postgraduate School. The manuscript was typed by Judy Kaitala.

Finally, a very sincere thank you to my wife Jana, for her understanding of many months of nightly separation and her assistance in the final frantic weeks of the manuscript preparation.

I. INTRODUCTION

The atmospheric boundary layer above land has been thoroughly studied and is well known. However, over the oceans, where the mobility of the underlying surface has to be considered, the investigation and knowledge of the structure and dynamics of this layer is still incomplete. Conflicts have existed in the theories describing the basic dynamic interaction between surface waves and the airflow above them.

Theoretical models, with valid, comparable observational results, are required to provide detailed descriptions of the structure and energy transfer mechanisms of the near surface layer over the ocean. Examples of geophysical problems in need of this information include: long-range atmospheric prediction models which require, for the near surface layer, a better specified input of the kinetic energy losses and the thermal energy gains and surface wave predictions requiring wind speeds at specified levels in the surface layer.

The primary purpose of this study is to perform joint probability analyses on velocity data obtained in the near surface layer and on simultaneous wave data. From these analyses, interpretations will be made on the phase-amplitude relationships, nonlinear properties, and some determination of the influence on turbulence present. These

results are compared to existing wind-wave coupling theories and to other observational results which have only recently compared favorably with these theories.

An inherent problem in the collection of meteorological data in the near surface layer over water waves in the ocean is the effect of the motions of the sensor platform. The data used in this investigation were accumulated using sensors mounted on a platform which, although relatively stable, did experience some motion in response to the waves.

A parallel purpose of this study will be to attempt to determine qualitatively, if not quantitatively, the effects of platform motion on the results from these specific analyses.

II. BACKGROUND

A. SEA-AIR INTERACTION EXPERIMENT

In May of 1969, the "Barbados Oceanographic and Meteorological Experiment" (BOMEX) took place in the Atlantic Ocean east-northeast of Barbados, West Indies. BOMEX was a joint investigation by several agencies and universities, including a team from the University of Michigan which collected the data used in this study. The overall purpose of BOMEX was to establish the energy budget of a volume 500 km square and 5 km above the ocean surface to 500 m below it.

As one of the largest environmental research programs ever conducted, BOMEX contained over 80 subprograms. Of particular interest to this study was the "sea-air interaction" subprogram. One aspect of this subprogram was to collect data in the near surface layer. Various oceanographic research platforms were used in these measurements. The University of Michigan measurements were taken from the Scripps Institution of Oceanography Floating Instrument Platform (FLIP) which was located near the center of the volume at approximately 16°N latitude and 57°W longitude. Bronson and Glasten (1968) have described FLIP in some detail.

B. THEORETICAL BACKGROUND

Theoretical investigations of wind-wave coupling have progressed from the quasi-laminar model proposed by Miles

(1957) to the recent turbulence models, such as formulated by Yefimov (1970). The close agreement between recent observational results and numerical solutions from recent wind-wave coupling models by Yefimov (1970), Reynolds (1968), and several others provided the primary motivation for the design of this study.

Most theoretical formulations of linear theory for wind-wave coupling have several common assumptions such as two-dimensional flow and a specified mean wind dependent only on height, and other common simplifications such as a single-component wave field and suitable linearized forms for the defining equations. A distinguishing feature of the formulations by Yefimov and Reynolds, and more recently by Stauffer (1973), has been the allowance for the interaction between the wave-induced motion and the turbulence in the overlying shear flow. In contrast to this, Miles (1957) neglected turbulence except for its role in determining a assumed logarithmic mean profile. Davis (1972) provides description and evaluation of the approaches in the more recent turbulence models.

Miles' theory is a quasi-laminar wave generating mechanism wherein the wave-induced motion is assumed to follow the potential flow theory. The existence of the critical level, which corresponds to the level where the wind speed is equal to the phase speed of the perturbing wave, is the key to Miles' theory. Below the critical level the airflow would appear to be opposite that of the

wave propagation since the wind speed is less than the phase speed of the wave. Above the critical level the wind speed exceeds the wave speed; hence the flow is opposite to that below but in the same direction as the wave. Miles' theory is based on the premise that waves only modulate the mean wind flow over them and that turbulence is not influenced; thus the Reynolds stresses are only dependent on the height above the mean wave surface. Figure 1 illustrates the phase and amplitude features of two components of the velocity and the stress uw , with respect to the wave as predicted by potential flow theory. These predictions apply to fluctuations observed at a fixed level in a shear flow above a progressive wave.

In Yefimov's formulation the allowance for turbulence in the airflow required the accounting of the nonlinear terms in the equations of motion. The model provides that dynamics at the critical level are not the only reason for wave related motion to deviate from potential flow predictions. Several features in Yefimov's solutions are due solely to the prescribed interaction between the prescribed motion and turbulence. As such, they occur independently of the height or of the existence of the critical level. These features were the variations with height of the phase differences between the velocity components and the wave.

C. OBSERVATIONAL BACKGROUND

Theoretical investigations of wind-wave coupling have seemingly progressed at a steady rate; however, until

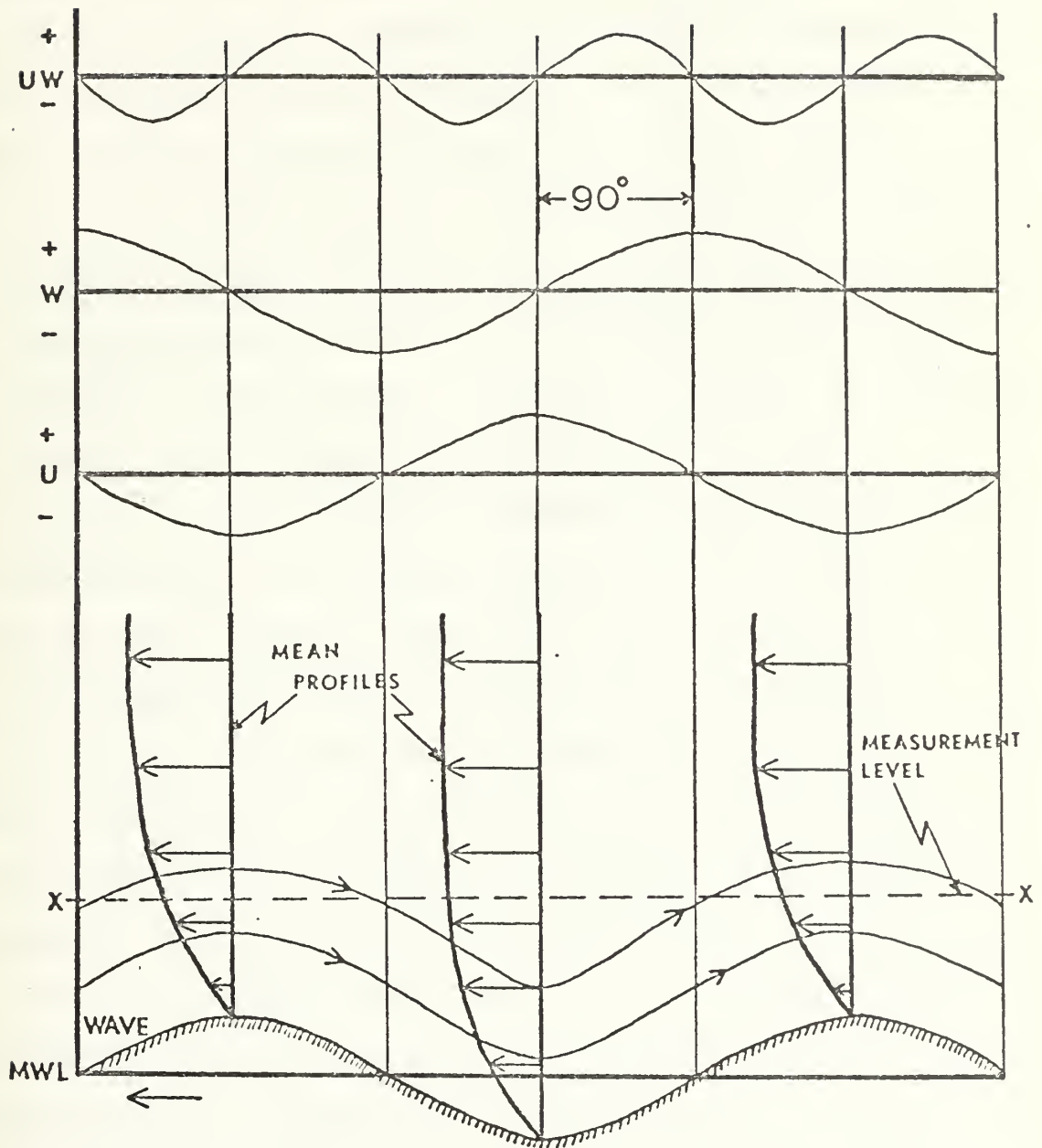


Figure 1. Phase-Amplitude Relations Predicted by Potential Flow Theory for the Two Components of Velocity (u and w) and the Stress uw , with Respect to the Wave (from Davidson and Frank, 1973).

recently the availability of overwater measurements has been insufficient to either verify or modify existing theories. Over the last six years the situation has improved considerably. Observational studies of measurements over natural waves in the near surface layer have been described by Davidson (1970), Pond, et al. (1971), Kondo, et al. (1972), Davidson and Frank (1973), Thompson (1972) and a number of others. Of particular interest to this thesis are the investigations of Davidson and Frank, and Thompson. Their studies are similar in types of analysis and features identified to those used in this study.

Davidson (1970) examined simultaneous measurements of velocity fluctuations and wave heights at two separate levels on Lake Michigan. These data were analyzed by spectral methods and showed rather clearly that the air-flow was being influenced by the underlying wave field. Davidson and Frank (1973) re-examined the Lake Michigan data using joint probability density-conditional mean analysis procedures. The earlier spectral results were compared to the wind-wave coupling predictions of Miles' theory while the JPDF-CMF results considered the role of turbulence in these same data. Recently the results of these analyses were used for comparison in a numerical turbulence model by Stauffer (1973). The model used by Stauffer is very similar to Yefimov's. The comparison of the velocity components, u and w , and the stress uw , showed agreement between the predicted values and those observed.

Thompson (1972) used essentially the same analysis procedures as those used by Davidson and Frank. In his analysis he used some periods of the same data analyzed in this investigation. Thompson interpreted JPDF-CMF based phase-amplitude results with respect to potential flow predictions and the role of turbulence in wind-wave coupling. He observed that the wave-related motions in the near surface layer were essentially nonpotential.

These two investigations are of primary interest in respect to this investigation for several reasons. Both investigations used analysis procedures which were the basis for those used in this study and therefore result in the same parameters for comparison. The Lake Michigan results, to which these results can be compared, are in agreement with those predicted by a numerical model. In addition, the Lake Michigan data were accumulated from a fixed instrument platform. Comparison of the results from this investigation with those from Lake Michigan should provide some indications as to the effects of a moving instrument platform. And finally, Thompson, in his analysis of BOMEX data, made minimal consideration for the possible influence of FLIP's motion on the results.

Thompson followed the analysis by Rudnick (1967) in neglecting the possible influence of platform motion on the results. Thompson indicated, on the basis of Rudnick's study, that his observed fluctuations in u and w were approximately 10^2 times larger than could be induced by platform motion.

However, Pond (1968) notes that there are marked differences between measurements from buoys and fixed masts. Pond states that provided some damping (by design or mooring) is done of the vertical motion and provided that the amplitude of the oscillating tilt is smaller than 10° - 20° , the effects of buoy motion are fairly small. He shows that if these conditions are met the effects of buoy motion are "probably" 10-20%.

Provided¹ in Appendix A is a fairly simple attempt at the representation of the apparent wind field in relation to a moving spar buoy. An attempt will be made in the presentation of results to use these representations, and the results of Rudnick and Pond to determine qualitatively the effect of FLIP's motion.

¹The descriptions in Appendix A were provided through personal consultations and correspondence with Dr. A. W. Green of the Department of Meteorology and Oceanography, University of Michigan.

III. DATA COLLECTION

University of Michigan personnel obtained 54 hours of data in 40 separate observational periods during the BOMEX experiment. Detailed descriptions of the sensors, sensor arrangement and mounting, and recording equipment are available in reports and studies by Portman, et al. (1970), and Thompson (1972). This information will only be briefly mentioned in the following paragraphs. An aspect of significant importance for this study is consideration of FLIP and its use as an instrument platform.

A. INSTRUMENTATION

Hot film, constant temperature anemometer systems were mounted at the 2, 3, 6, and 8 meter levels on the vertical mast (See Figure 2). These sensors were capable of measuring the three fluctuating velocity components (u , v , and w) at each level.

A resistance wave gage, provided by Dr. R. E. Davis, Scripps Institution of Oceanography, was used to measure wave heights. The wave gage was positioned about five meters inboard of the vertical instrument mast.

B. FLOATING INSTRUMENT PLATFORM (FLIP)

In the previous section the motions of the spar buoy, such as FLIP, were discussed from a general, theoretical standpoint. The following paragraphs are a more specific

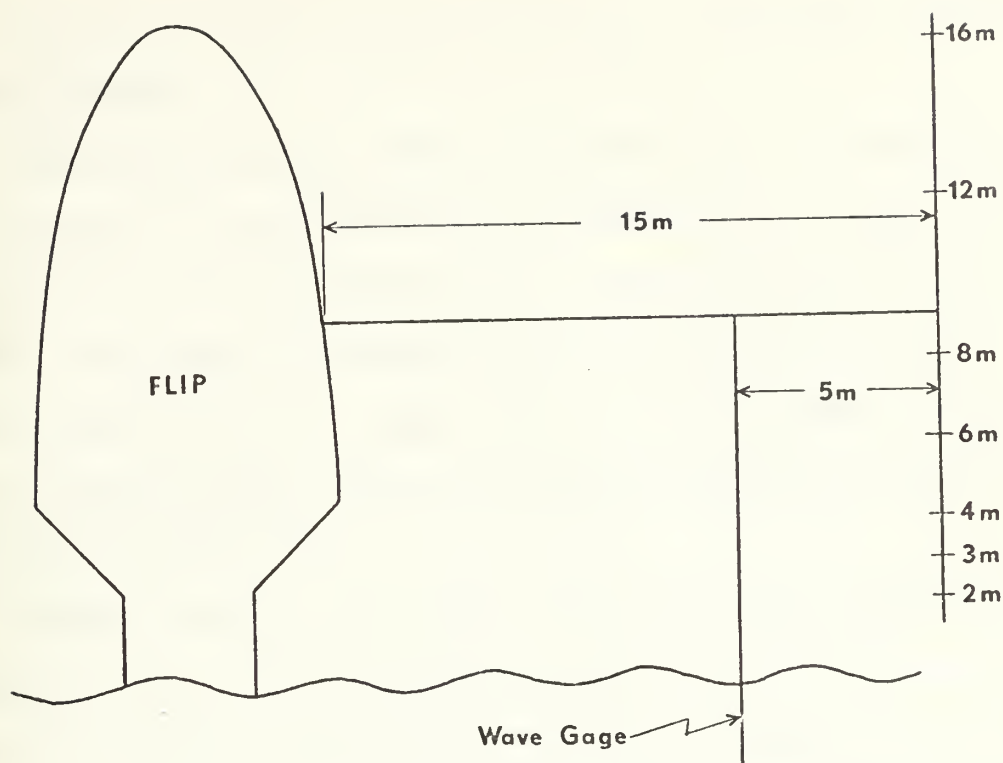


Figure 2. View of FLIP Showing the Arrangement of Sensors during BOMEX.

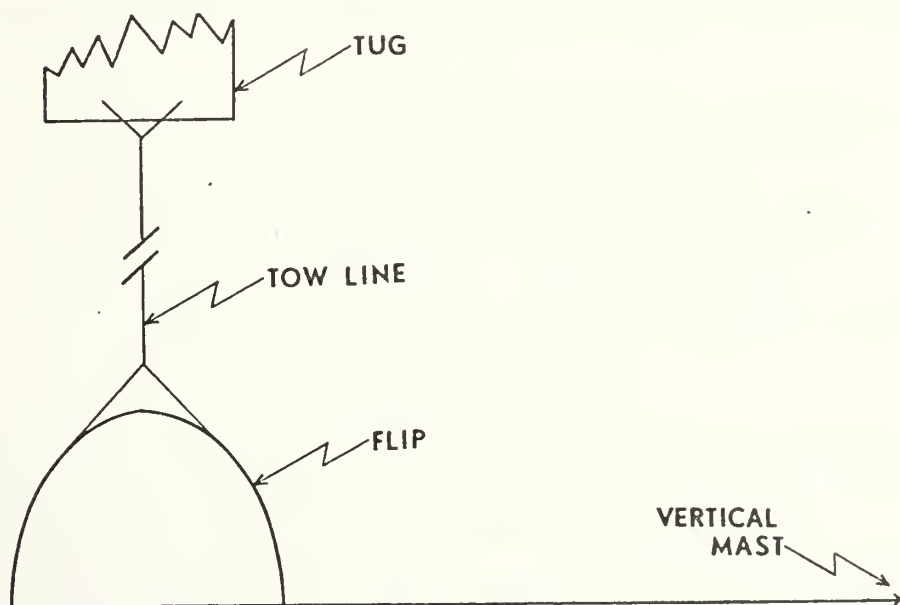


Figure 3. Top view of FLIP Showing the Mooring Procedure Employed during BOMEX.

description of FLIP and its use as an instrument platform during BOMEX.

Möller-Christensen (1968) reported that a minimum of distortion to the natural wind flow by FLIP's super-structure would occur if the deck of FLIP were positioned into the wind. This was determined in wind tunnel tests using a scale model of FLIP. Möller-Christensen recommended that the vertical sensor mast be positioned about 15 meters outboard of the hull.

Figure 3 shows the method utilized during BOMEX to maintain FLIP's position with respect to the wind direction. The tug was positioned about 800 meters downwind of FLIP. The tug was unable to maintain constant tension on the towing cable and this has been discussed by Superior (1969). As a result of a varying tension on the towing cable and the positioning method in general, axial and lateral motions of FLIP occurred.

Unfortunately, real time measurements of FLIP's motion, due to the features described above and those caused by wave motion, are not available. Because of this it is doubtful that the exact effects of FLIP's motion on the data collected can be accurately described.

Another problem of concern to data interpretation was that provisions were not available during BOMEX for adjusting the vertical position of the sensor mast, independent of FLIP's motion. This caused the sensors to be out of level during a portion of each period.

IV. THE PREPARATION AND ANALYSIS OF DATA

Joint probability density--conditional mean (JPDF-CMF) analyses were used to identify features in the fluctuating velocities which were associated with the waves' presence. Phase-amplitude results were then based upon the JPDF-CMF analysis.

In general, the procedures used in the analysis of the data for this study were the same as those originally described by Holland (1973) and applied to these kind of data by Thompson (1972). Improvements were made in the procedures for defining phase-amplitude information from the JPDF-CMF analyses. The resolution of the phase-amplitude results was increased to enhance the shape and phase relationships of the curves.

A. INITIAL DATA PREPARATION

Several basic data processing steps¹ preceded the application of the JPDF-CMF analysis procedures. These included digitizing, application of an analog filter, time corrections, scaling of data to engineering units, and several other procedures described in adequate detail by Bingham (1972). An iteration of the details of these preliminary steps will not be included in this report.

¹Initial data preparation procedures were developed by the Department of Meteorology and Oceanography, University of Michigan, under the direction of Professor D. J. Portman.

B. BAND PASS FILTERING AND NORMALIZATION

In order to remove high and low frequency contamination and to focus the analysis on fluctuations near the frequency band corresponding to the water waves, a band pass numerical inverse transform type filter was applied to all data. This type of filter could be very useful in also removing low frequency contamination to the data from FLIP's motion. The filter was designed on the basis of available spectral results and had a frequency band with 0.1 and 0.8 Hz as the low and high cut-off frequencies, respectively. The filter's response curve appears in Figure 4.

Prior to application of the JPFD-CMF procedures the data were normalized by dividing the deviation from the mean by the standard deviation.

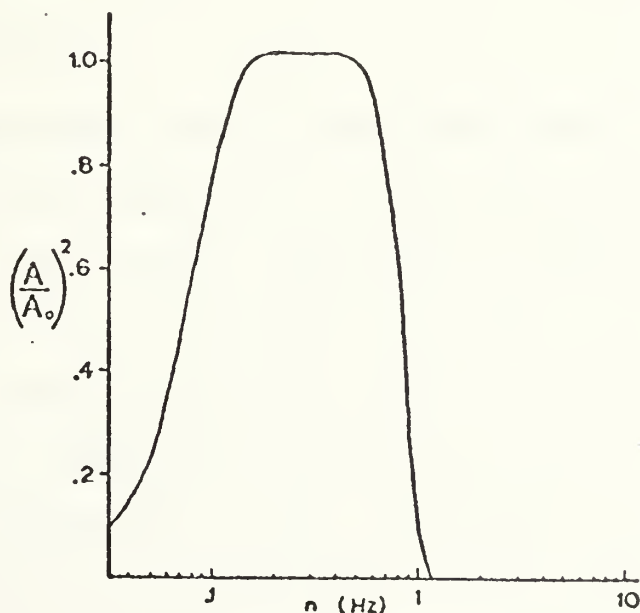


Figure 4. Response Curve of the Band Pass Numerical Inverse Transform Filter.

C. JPDF-CMF PROCEDURES

The particular procedures used in the JPDF-CMF computation were developed from descriptions by Holland (1973). A brief but complete discussion of these procedures is given by Davidson and Frank (1973) and Thompson (1972). The JPDF-CMF computational procedures, when applied to three variables, result in the joint probability density function (JPDF) for a pair of variables with the conditional mean of a third variable as a function (CMF) of the first two variables. Representation of the resulting trivariate statistical relationship and further discussion of the JPDF-CMF analysis are contained in later sections. The JPDF-CMF computations were made from the normalized values of the original variables sampled at five points per second, with a majority of the records consisting of 6062 points or approximately 20 minutes of data.

D. PHASE-AMPLITUDE COMPUTATIONAL PROCEDURES

While various features of the fluctuations in the airflow above water waves can be identified by JPDF-CMF analysis, a simplification of the method of display is desirable in order to concentrate attention on the essential variations and eliminate redundant background information. For this study, the emphasis is on the statistical dependence of turbulent variables on the phase of some reference variable. Based on JPDF-CMF procedures, Holland (1973) described a method to determine this phase-amplitude information.

Polar coordinates representing the amplitude and phase angle of a variable such as the wave height (η) can be determined from the JPDF array for the variable, η , and its time derivative, $\dot{\eta}$. In amplification, any conditional mean function of η and $\dot{\eta}$ is a CMF of the phase and amplitude of the η fluctuations because for each value of the dependent variable represented by the CMF, the coordinates in $\eta, \dot{\eta}$ space are determined by the amplitude of the η fluctuation occurring at that time and by the phase angle within that fluctuation. As an example, the conditional mean function $w(\eta, \dot{\eta})$ would illustrate the dependence of the vertical component of wind velocity on the phase and amplitude of the wave.

An example of the JPDF-CMF array and the resulting phase-amplitude curves appear in Figures 5 and 6. Indicated on the array are the numbered 30° segments and the class limits which were used to approximate the 1.5σ circle. The small amplitude class (amplitude $< 1.5\sigma$) contains about 3/4 of the observations and the large amplitude class (amplitude $> 1.5\sigma$) contains about 1/4. Selection of these class limits is somewhat arbitrary. The phase is defined in terms of the 30° segments measured counterclockwise in the $\sigma_{\dot{\eta}}, \sigma_{\eta}$ coordinate system (JPDF-CMF array) from the positive $\sigma_{\dot{\eta}}$ axis.

Using Figure 5 as an example, the following procedures were used to obtain the resulting phase-amplitude curves.

[1] Lower figures (JPDF array) in each joint class interval are summed over each 30° segment and amplitude class. The

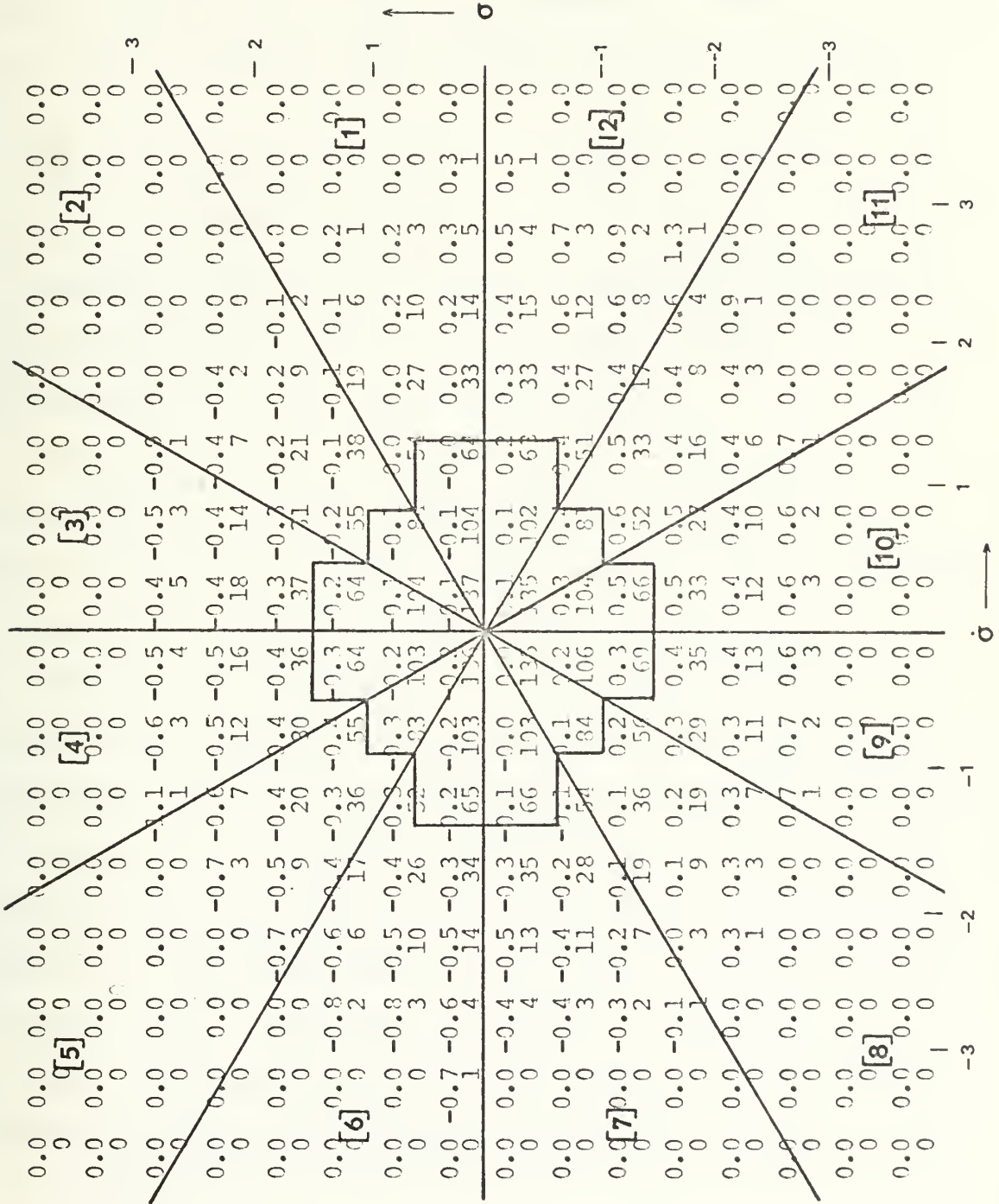


Figure 5. Two-Dimensional JPDF-CMF Array.

joint densities in joint class intervals along the segment lines are divided by percentages and are added into the segments which share these joint intervals. Each probability sum is then divided by the sum over the entire amplitude class.

[2] Products of the dependent variable (CMF) and probability density (JPDF) in all joint intervals of each 30° segment and amplitude class are summed and the sum is divided by the total probability in that segment and amplitude class.

Results of these procedures yield a single curve for each dependent variable, showing it as a conditional mean function of the phase angle of the reference variable, which is also illustrated as a single curve (Figure 6).

Previously, investigators using these procedures (Davidson and Frank, 1973, and Thompson, 1972) performed the summations over octants (45° segments). In this study, using 30° segments, a considerable improvement over the previous studies in the resolution of the phase-amplitude curves was achieved. Phase-amplitude results using octants are shown in Figure 7 for comparison with those in Figure 6.

Additional aspects of the phase-amplitude results are presented during a discussion of results.

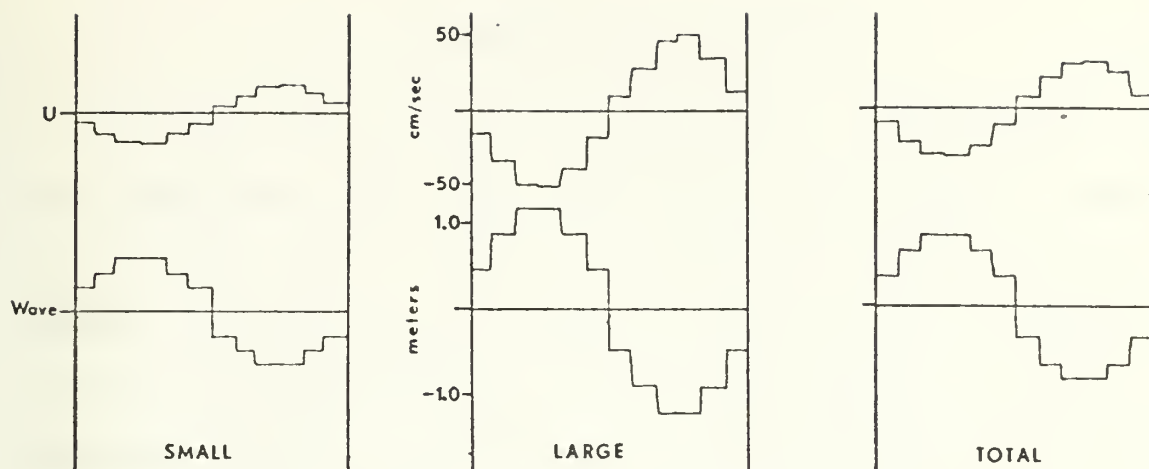


Figure 6. Phase-Amplitude Results Showing the Resolution Achieved by Summing over 30° Segments.

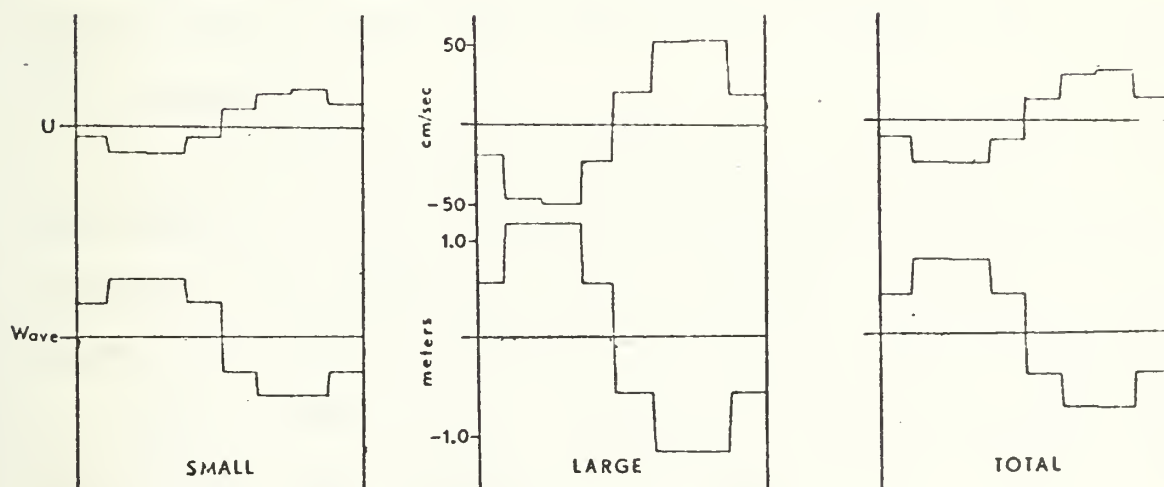


Figure 7. Phase-Amplitude Results Showing the Resolution Achieved by Summing over 45° Segments as used by Previous Investigators.

V. PRESENTATION OF RESULTS

The data from 14 periods were analyzed during this investigation. They were collected on five separate days and represent over 15 hours of observations during BOMEX. The periods were from 34 minutes to 80 minutes in length. Analyses were performed on data from the three, six and eight-meter levels with one period consisting of simultaneous data from both three and eight meters. For the purposes of JPDF-CMF and phase-amplitude analyses, each period was divided into subsets (2 to 4), each of which was 20 minutes or less in length. The last subset in each period was usually less than 20 minutes long. Table I gives a summary of all periods analyzed, indicating times of observation, height analyzed, mean wind speed at that height, and several other parameters.

General meteorological conditions, wave heights, and corresponding times as reported by University of Michigan personnel during BOMEX are given in Figure 8. The general atmospheric conditions during all periods could be described as stable or near neutral. Profiles of wind and temperature measurements from two meters to 16 meters can be found in a study by Superior (1969). There were no periods of active wave growth or rapid decay. The conditions for the area in which FLIP was located could be described as a region of light to moderate winds into which swell was propagating. Thus it was fairly representative of the surface layer over the ocean and relevant to this discussion.

Table I. Summary of Analyzed Periods

Period Number	BOMEX Number	Date (1969)	Time (GMT)	Height Analyzed (m)	Wind Speed (mps)	U* (mps)	Wave Heights (ft)	Phase Speed (mps)	C/U*
1	A-10	19 May	0308-0429	6	10.4	.28	6-8	13.5	48.1
2	A-11	19 May	0546-0708	6	9.3	.33	6-8	13.6	41.2
3	A-12	19 May	0754-0829	6	9.8	--	6-8	--	--
4	A-16	19 May	1843-2003	8	9.5	.26	6-8	15.1	58.0
5	A-17	19 May	2110-2150	8	9.2	.25	6-8	14.4	57.6
6	A-18	24 May	2020-2125	8	7.0	.12	3-5	14.6	130.3
7	A-22	26 May	1432-1506	8	6.4	.17	4-6	13.7	80.5
8	A-23	26 May	1706-1742	8	6.6	.16	4-6	16.2	101.5
9	A-26	27 May	0501-0554	8	8.4	.31	3-6	15.1	48.8
10	A-27	27 May	0901-1023	8	8.6	.28	3-6	14.6	52.2
11	A-28	27 May	1058-1220	8	8.2	.37	4-7	15.7	42.2
12a	A-30	27 May	1616-1738	8	10.0	.25	7-11	15.4	61.6
12b	B-30	27 May	1616-1738	3	9.8	.20	7-11	15.4	76.9
13	A-35	28 May	0934-1055	8	8.0	.11	6-10	14.2	128.8
14	A-39	28 May	1754-1916	3	7.6	.18	6-8	15.6	86.9

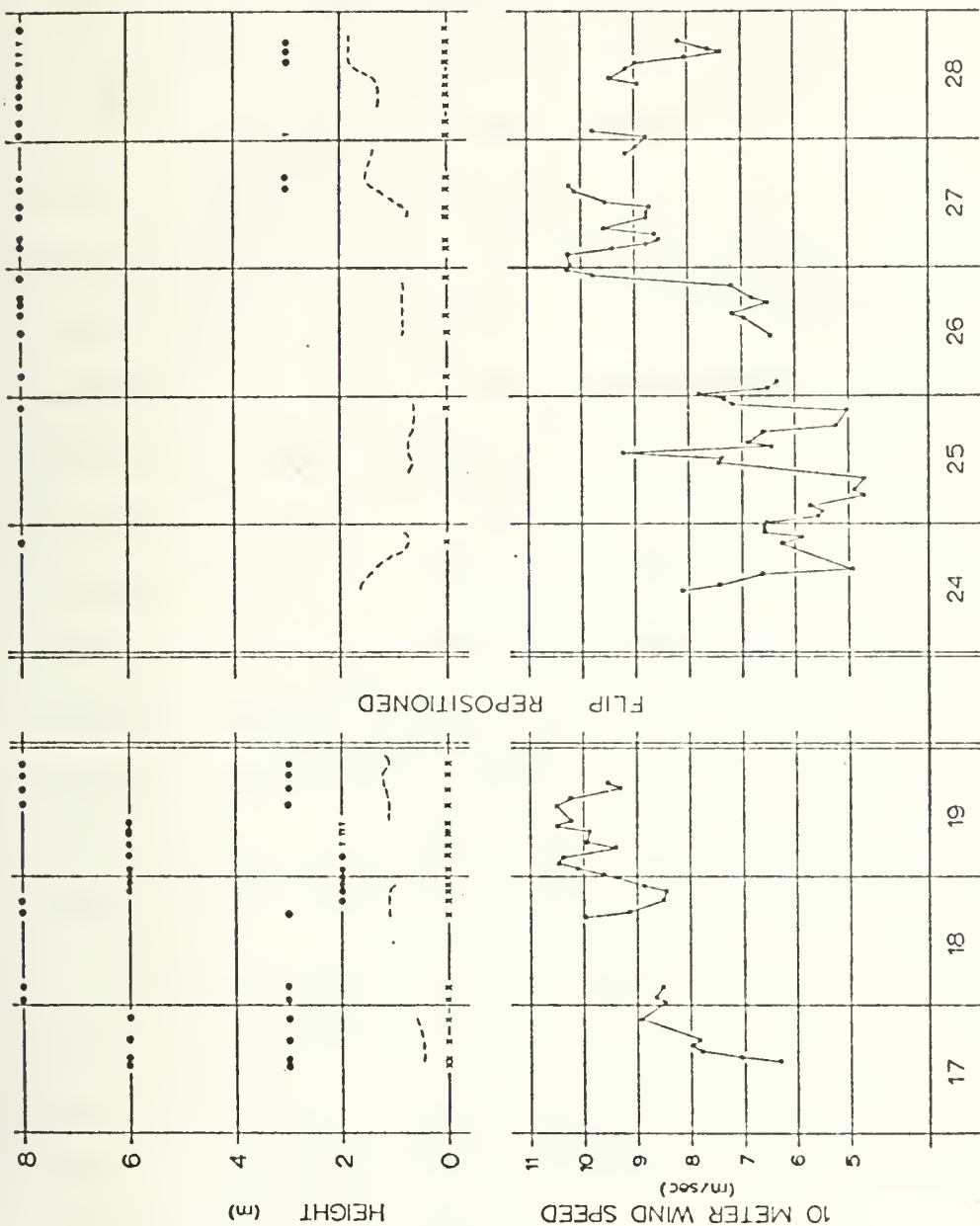


Figure 8. Measurements and Wind and Wave Conditions.
 Upper half: The symbols and letters show heights and times of
 University of Michigan measurements aboard FLIP.
 . - u, v, w, T; T - T only; x - waves; ----- visual estimates
 of wave height.
 Lower half: Average wind speed at 10 meters.
 (From Portman et al., 1970).

The results of the analyses of the period numbers marked with an asterisk in Table I will be those interpreted in detail in the following paragraphs, and include period numbers 1, 6, 12a, 12b, and 14. Results from these particular periods were chosen for several reasons. Periods 1 and 6 represent very nearly the extremes in observed mean wind speeds, while periods 6 and 12 represent the extremes in observed wave heights. Periods 12a and 12b, 8 and 3 meter level results, respectively, were also chosen because they were the only multiple level measurements available and, hence, can be interpreted with respect to phase-amplitude changes with height. They also should illustrate to a greater extent the effects of FLIP. Period 14 data was collected at the 3 meter level and had winds and wave heights between the extremes. This period corresponds to period 3 discussed by Thompson (1972) in which the motions of FLIP were essentially neglected but herein will be re-examined with consideration of sensor platform motion.

Data considered in the analyses were the u, v, and w velocity components, the stress uw, and the wave heights. Associated with each of these variables is a parameter τ_o , which is defined as the "statistical eddy period" and is determined by the ratio

$$\tau_o = 2\pi\sigma/\dot{\sigma} ,$$

where σ and $\dot{\sigma}$ are the standard deviations of the variable and its derivative. An indicator of the appropriateness of the

analysis is to compare τ_0 's for the dependent variable (u, v, etc.) with that of the reference variable, the wave height. If the statistical eddy periods differ significantly, the phase-amplitude information for the reference variable has a greater possibility of only representing the mean of numerous random fluctuations. Statistical eddy periods are listed on each of the figures depicting the results and do, in fact, attest to the validity of the analysis. The statistical eddy period for the product uw is less than that for the wave because uw in a linear system, at least, would appear as a second harmonic. For this reason, τ_0 is not listed for uw.

Acceptance is given, in the interpretations of the phase-amplitude results, to Kendall's (1970) suggestion that non-sinusoidal wave forms are evidence of non-linearities and, hence, a non-negligible role for turbulence. It should be noted that the "critical" level was found to be above 10 meters for all periods. In the following paragraphs descriptions of the periods discussed above are given in detail.

A. PERIOD 12

This period is unique in that it is the only period available from the data examined that contained simultaneous information from two levels and, as such, accounts for a major portion of this section.

The duration of the period was about 80 minutes and, hence, four subsets are available for each level. Wave

heights and wind speeds were observed (Figure 8) to have been increasing in the four to five hours preceding this period and reached a peak just prior to or in the early portion of the period. The wave heights for the period were observed to have been approximately seven to 11 feet with mean wind speed of 10.0 M/sec at the 8 meter level and 9.8 M/sec at 3 meters.

Figures 9 through 12 contain the phase-amplitude results from the 8 meter level while Figures 13 through 16 depict the 3 meter level. Only the phase-amplitude relationships of u , w , and the wave will be discussed in detail.

The u components at both levels and for all subsets during the period are surprisingly similar. The phase of the u component relative to the wave in all cases is as would be predicted by potential flow theory except that the extremes of u have shifted back slightly. Potential flow predicts, as shown in Figure 1, that u and the wave should be exactly 180° out of phase with each other. The phase shift observed in these results shows u to be trailing the crest or trough of the wave by about 15° to 30° . This shift was observed by both Davidson and Frank (1973) and Thompson (1972) and they associated the shift with momentum transfer. The amplitudes of the u component fluctuations decreased slightly from 3 to 8 meters.

The phase relationships in w are the most interesting of the results from this investigation. Between the 3 and 8 meter level there is a phase change for w of between 90°

(Figures 11 and 15) and 150° (Figures 9 and 13). As can be seen for the 8 meter level, the phase relationships of w with the wave and u are not consistent with potential flow theory with the possible exception of subset 3 in Figure 11. Some evidence is found to indicate the role of turbulence in that the wave-forms of w appear to be non-sinusoidal in subsets 1, 2, and 4 (Figures 9, 10, and 12). The fact that the u and w components at the 8 meter level are nearly in phase was also noted by Thompson (1972) and was attributed to turbulent interaction with the wave-induced motion. In subset 4 (Figure 12) it can be seen that there are no phase differences between u and w at the negative extrema; however, at the positive extrema w is leading the u by about 30° . Potential flow theory predicts that u and w would be in quadrature as indicated in Figure 1.

Non-sinusoidal wave-forms are also evident for the 3 meter level as seen in Figures 13, 15, and 16. At this level the departure of the vertical fluctuations from potential flow are most noticeable. Instead of being in quadrature as predicted, u and w are almost 180° out of phase. The maximum w fluctuation occurs when u is a minimum. This shift in w was also noted by Davidson and Frank (1973) in the results of their period 2 at the 1.5 meter level. They attributed this shift in the w component to "critical level" dynamics as a prediction in the quasi-laminar theory. However, with a change in the phase of w with height it can

be assumed that it was caused by turbulent interaction in this case.

This period provides some evidence that perhaps FLIP's motion did not appreciably affect these results. First, since FLIP is a rigid body and the vertical sensor mast is solidly attached, errors introduced by FLIP at one level would also be introduced at the other level. In other words, the fluctuations introduced by FLIP at one level would also be evident at the other and thus no phase shift could occur unless it was present in the airflow. From the discussion in Appendix A, FLIP could be considered an amplifier under certain conditions and, as such, could introduce phase shifts into the results. However, since the results at 3 meters are in agreement with the results at a lower level from a fixed platform (Davidson and Frank, 1973), this possibility will not be considered. FLIP may introduce some error into the magnitudes of the various fluctuating variables. However, it is doubted that that error could be determined from these results.

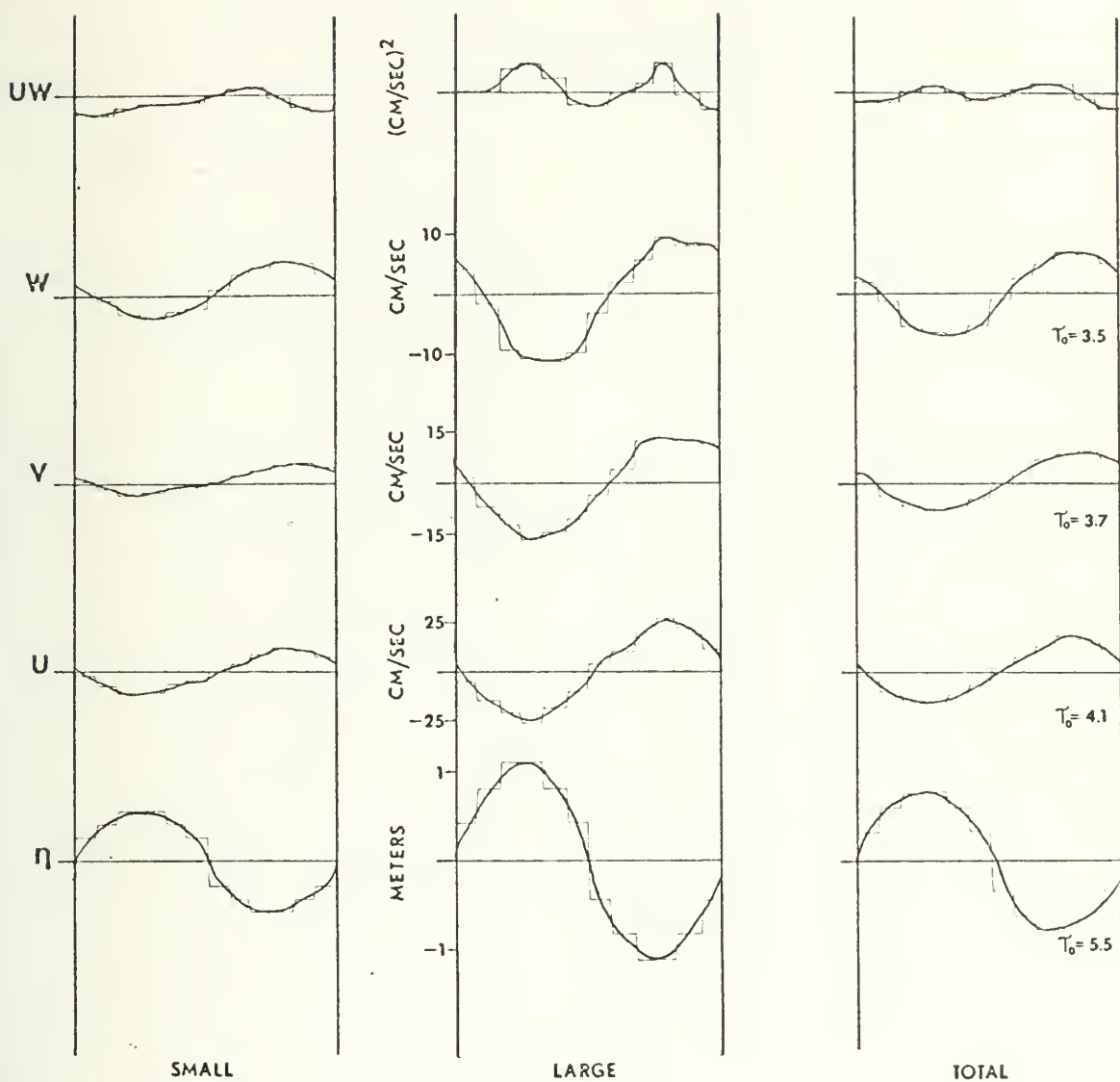


Figure 9. Phase-Amplitude Results for Period 12a, Subset 1 (8 meter level).

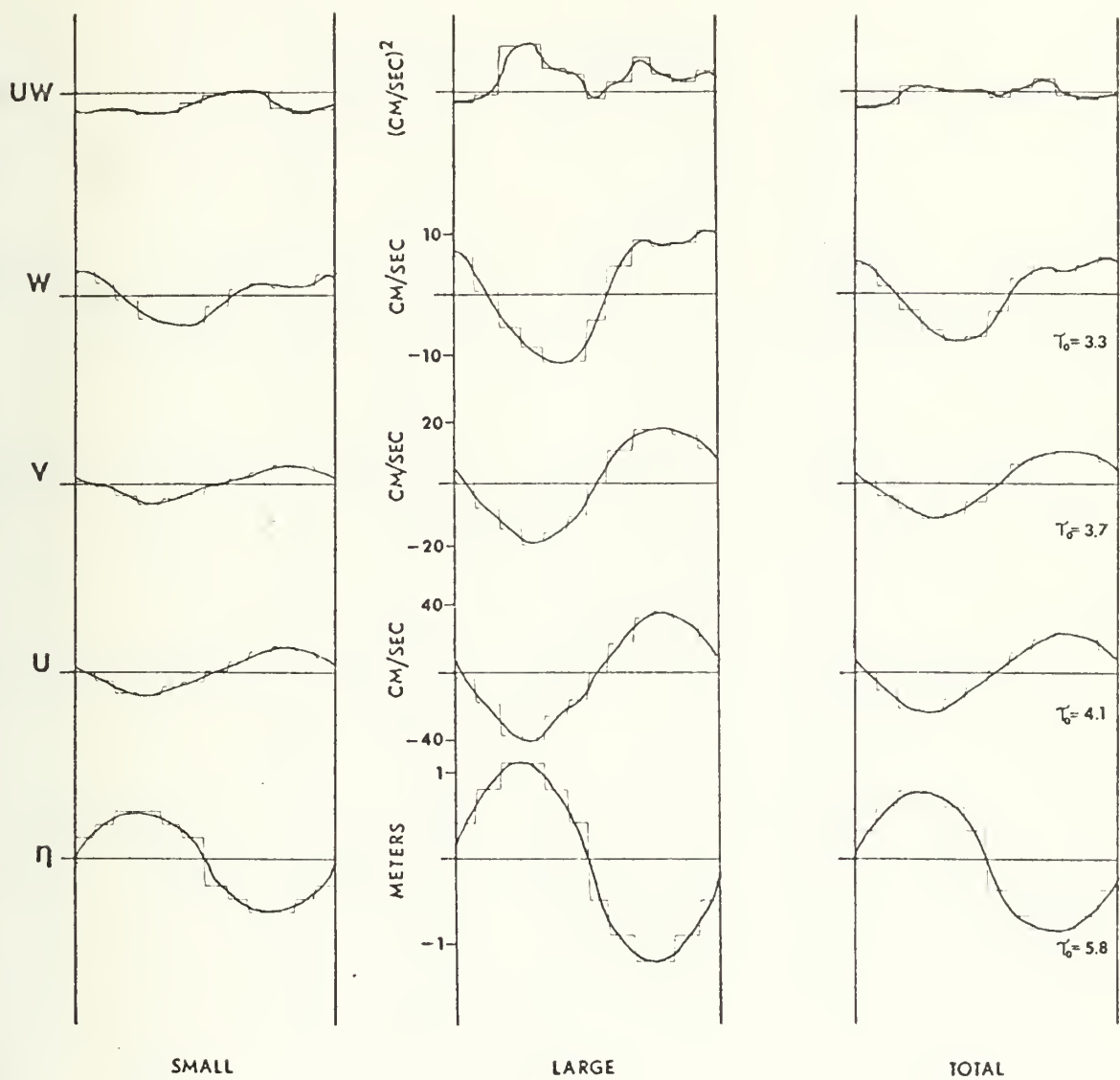


Figure 10. Phase-Amplitude Results for Period 12a, Subset 2 (8 meter level)

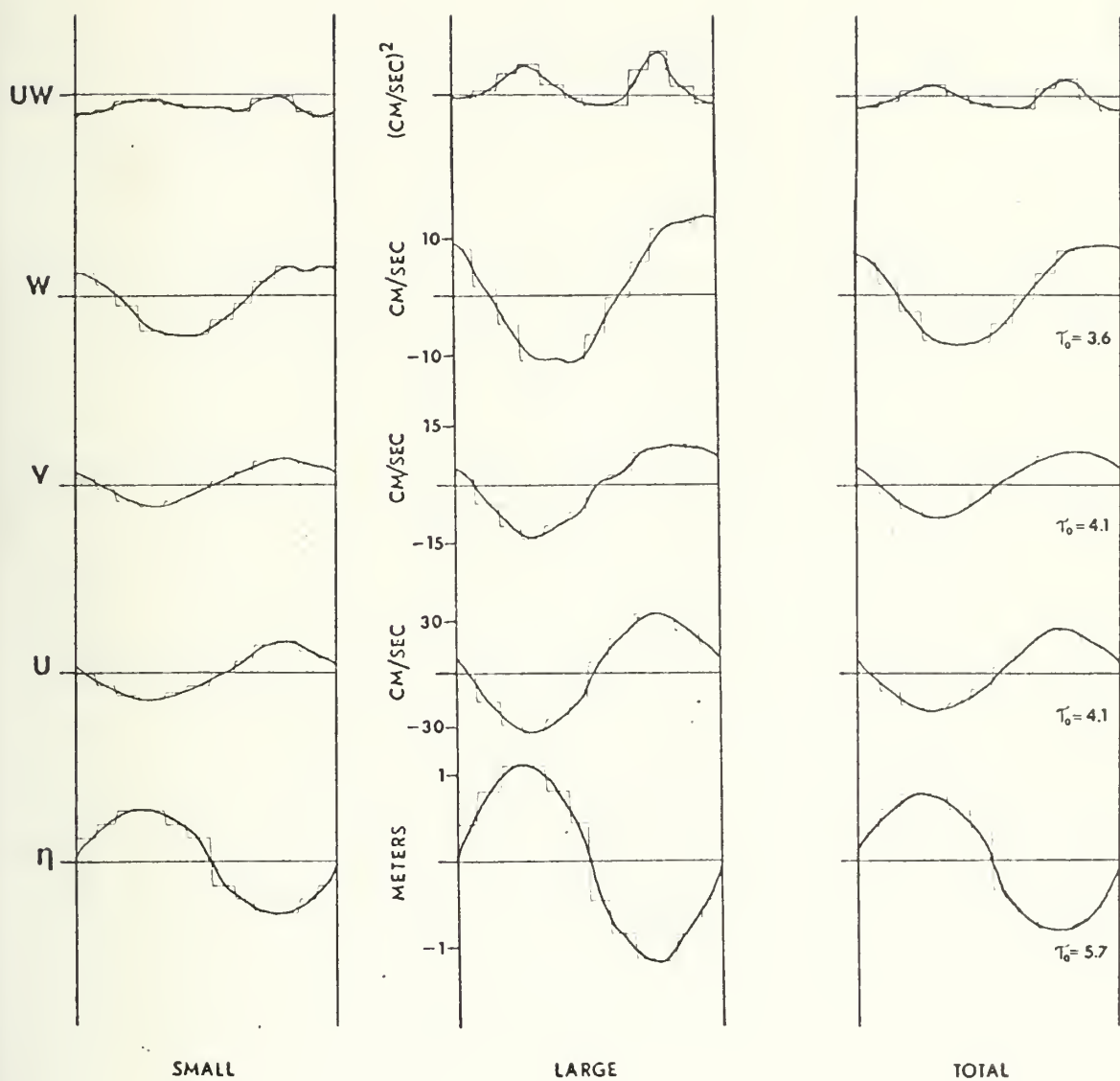


Figure 11. Phase-Amplitude Results for Period 12a, Subset 3 (8 meter level).

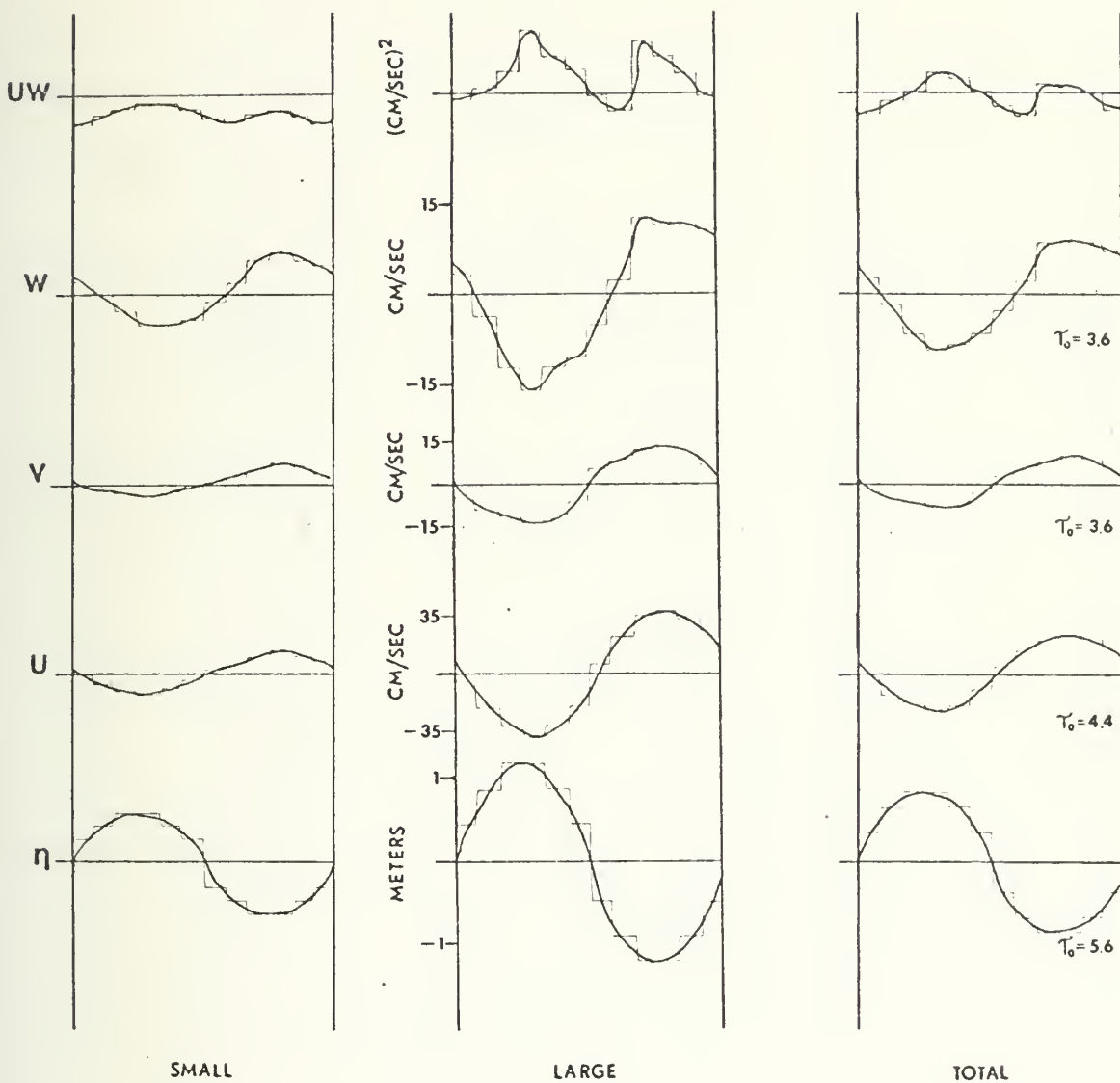


Figure 12. Phase-Amplitude Results for Period 12a, Subset 4 (8 meter level).

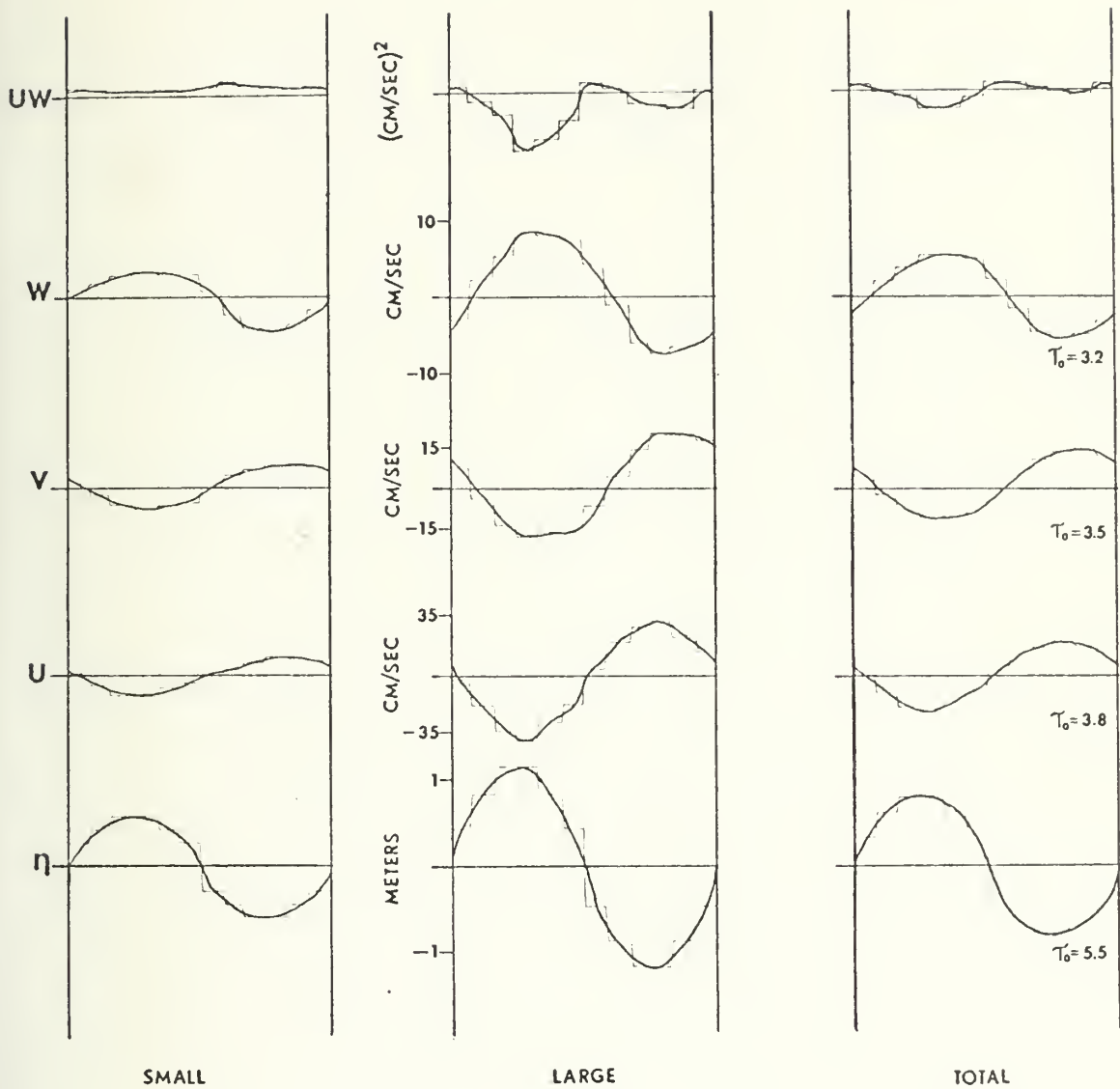


Figure 13. Phase-Amplitude Results for Period 12b, Subset 1 (3 meter level).

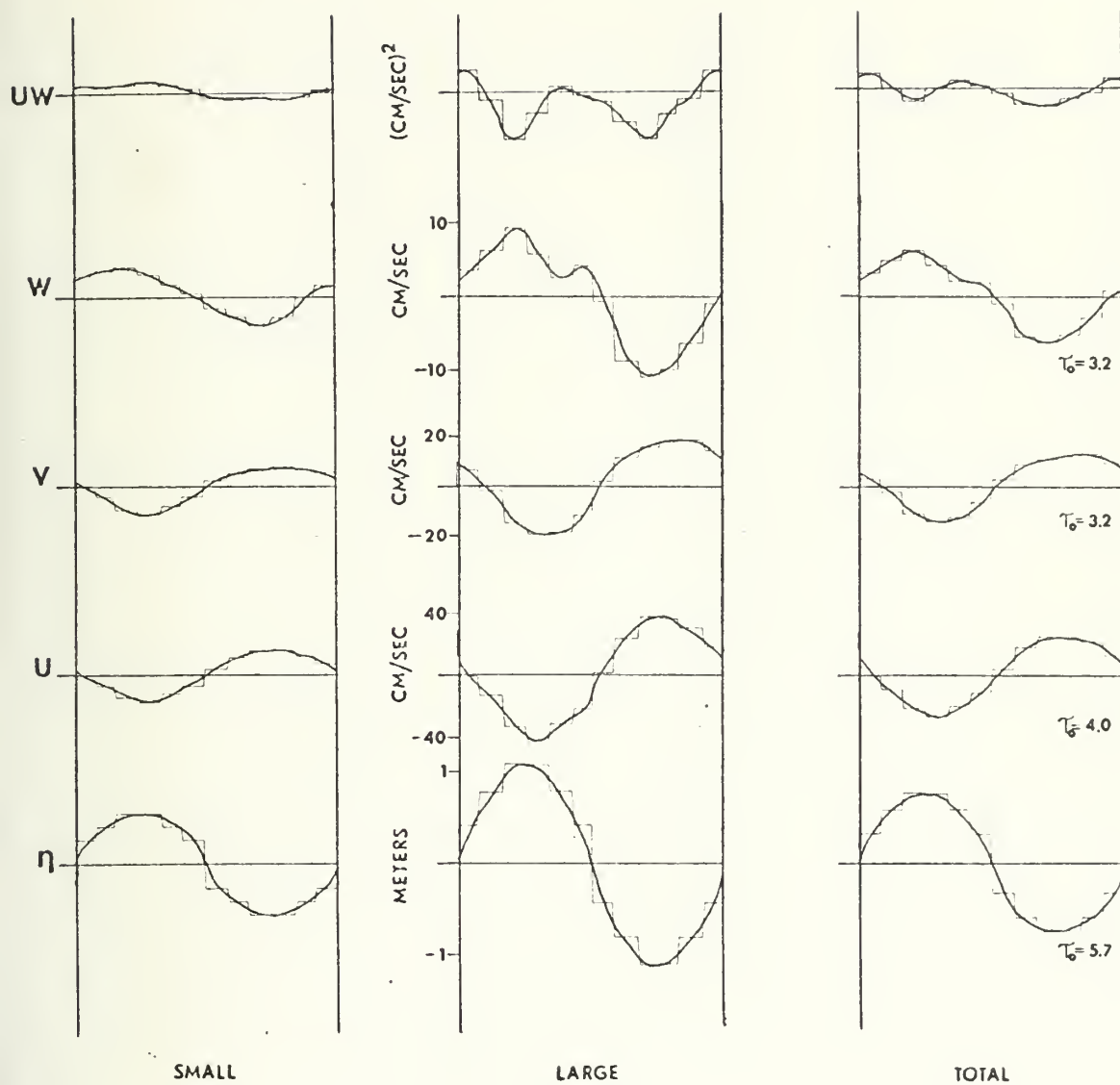


Figure 14. Phase-Amplitude Results for Period 12b, Subset 2 (3 meter level).

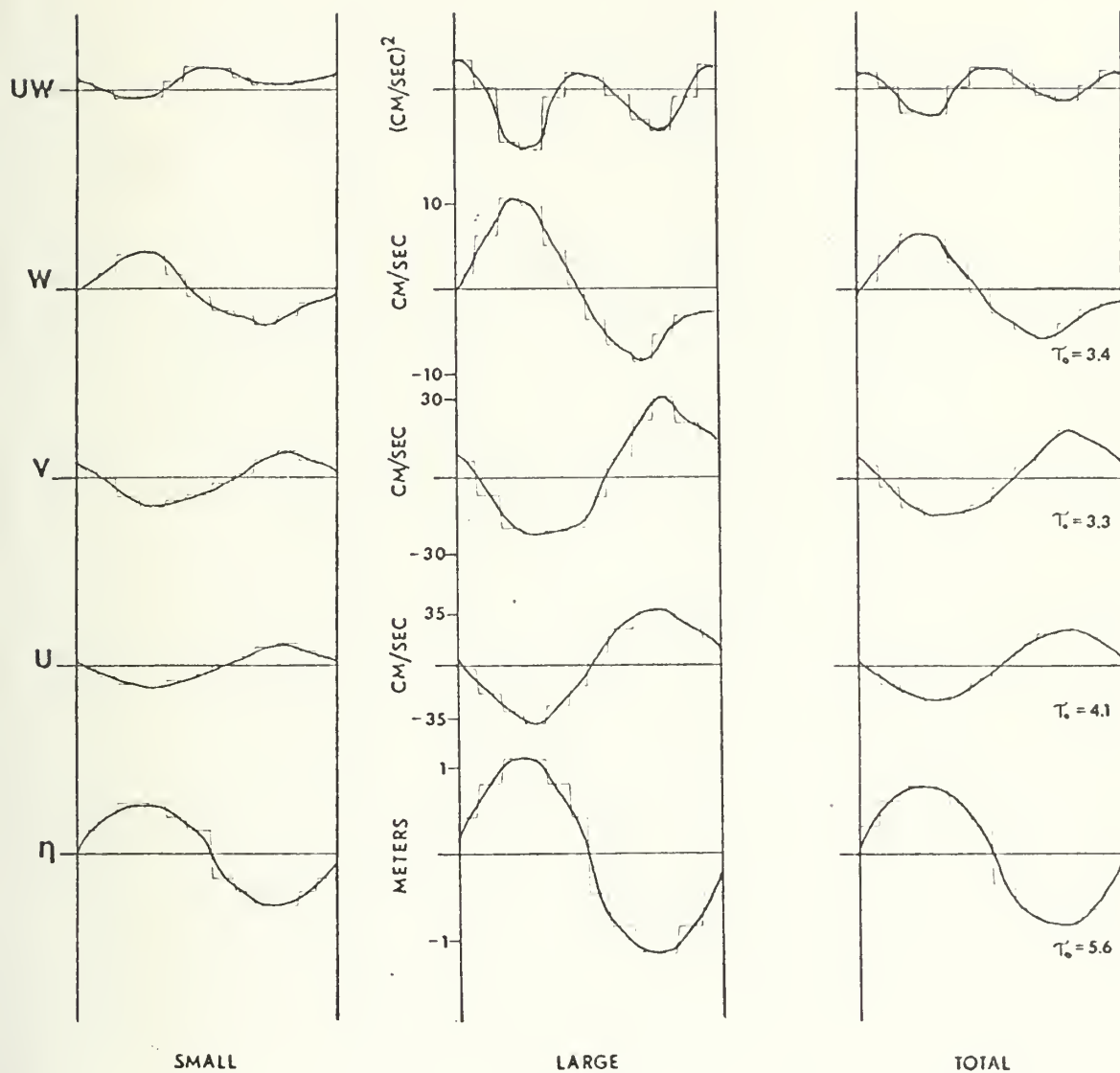


Figure 15. Phase-Amplitude Results for Period 12b, Subset 3 (3 meter level).

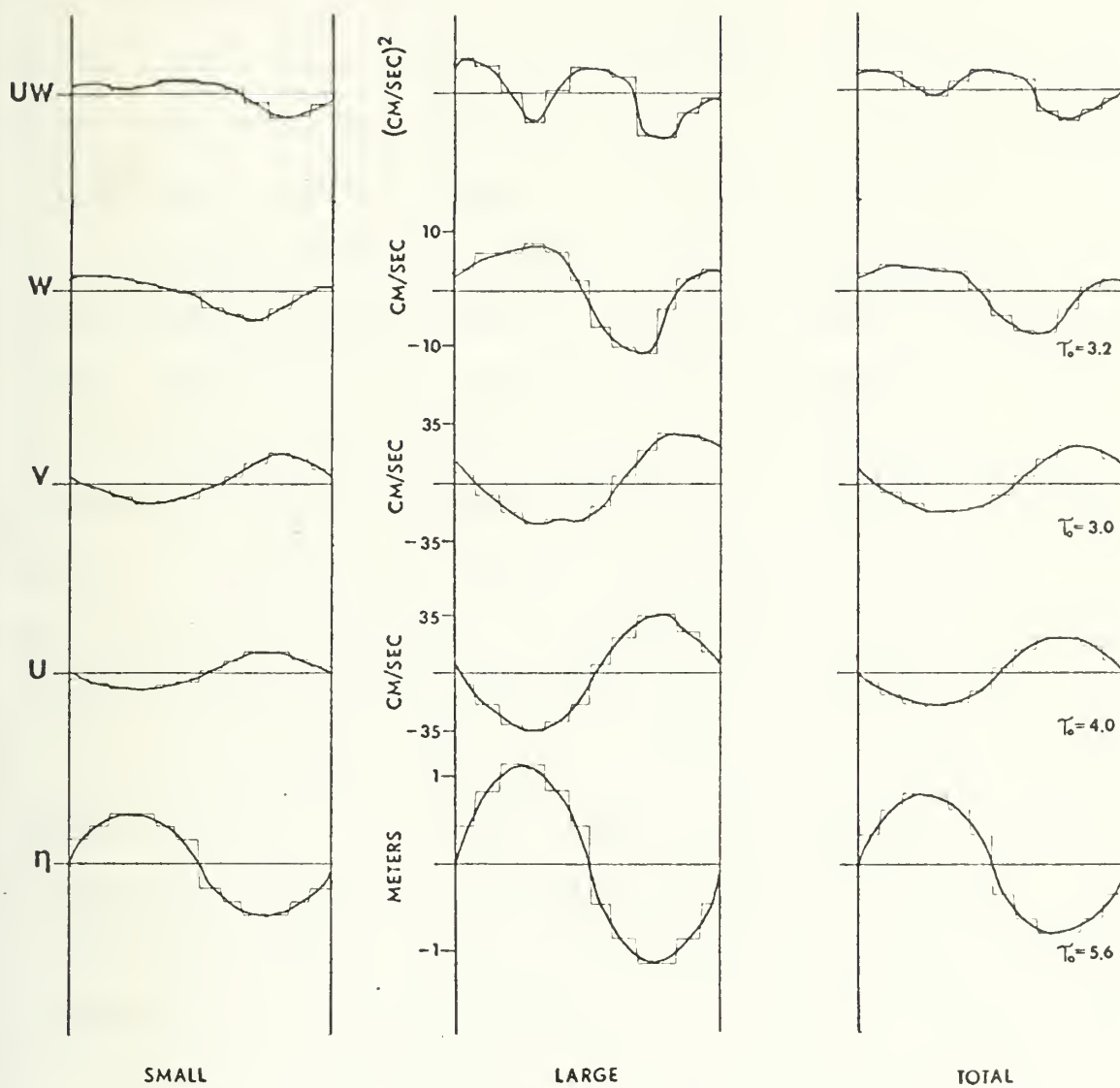


Figure 16. Phase-Amplitude Results for Period 12b, Subset 4 (3 meter level).

B. PERIOD 1

The highest mean wind speed of any period examined was observed during period 1. Observations were made at the 6 meter level. Wave heights were between six and eight feet, with a mean wind speed of 10.4 M/sec. This period is characterized by a complete departure from potential flow predictions.

The phase-amplitude results for u , though basically sinusoidal in subsets 1 and 2, Figures 17 and 18, show a larger shift back over the upwind side of the wave crest than had been observed in period 16. The shift is still present in subset 3 (Figure 19), and to a lesser extent in subset 4 (Figure 20); however, the shape of the wave-form has become non-sinusoidal. The amplitude of the horizontal fluctuations are observed to be relatively small.

A non-negligible role for turbulence is evident throughout the period for w . The wave shape of the vertical velocity fluctuations varies in all subsets of the period and sinusoidal forms are not observed. The amplitude of the w component is sharply diminished from all other periods examined.

The wave-related stress (uw) varies considerably over the period. Phase changes of up to 90° are observed from subset 1 to subset 4.

This distinct departure from potential flow, indicated by the non-sinusoidal shapes observed in the results of this period, could be due to non-linear processes.

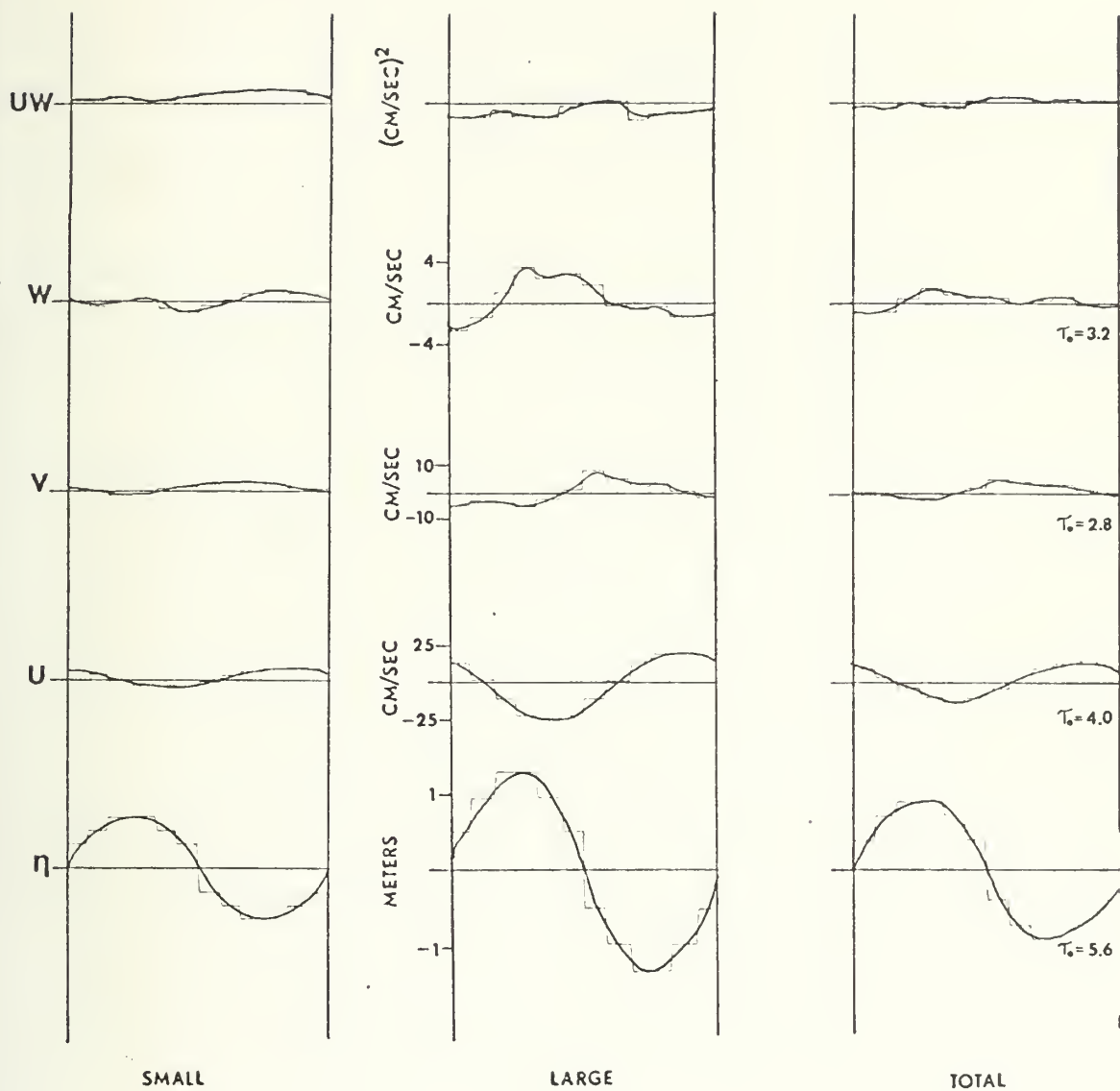


Figure 17. Phase-Amplitude Results for Period 1, Subset 1.

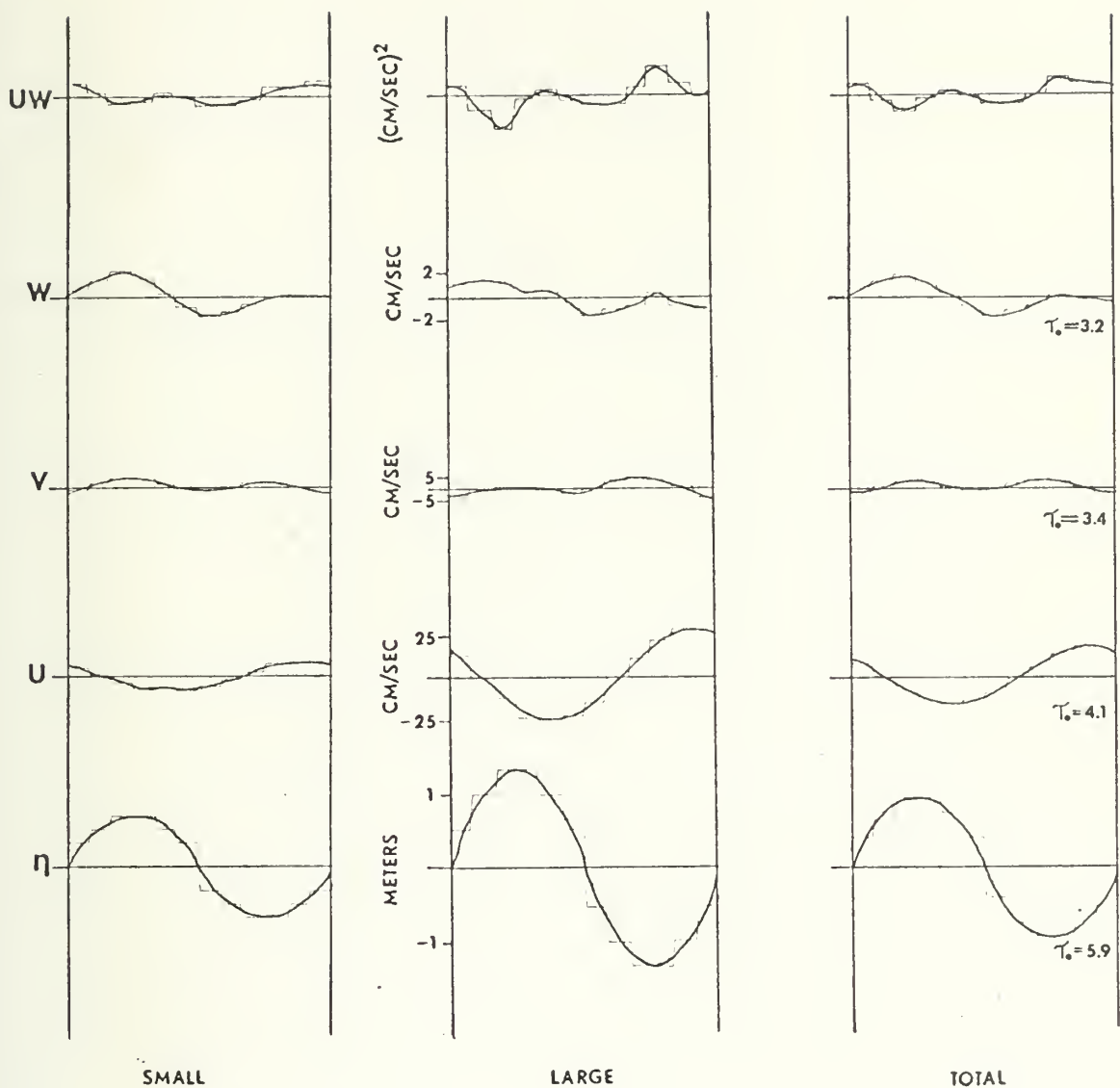


Figure 18. Phase-Amplitude Results for Period 1, Subset 2.

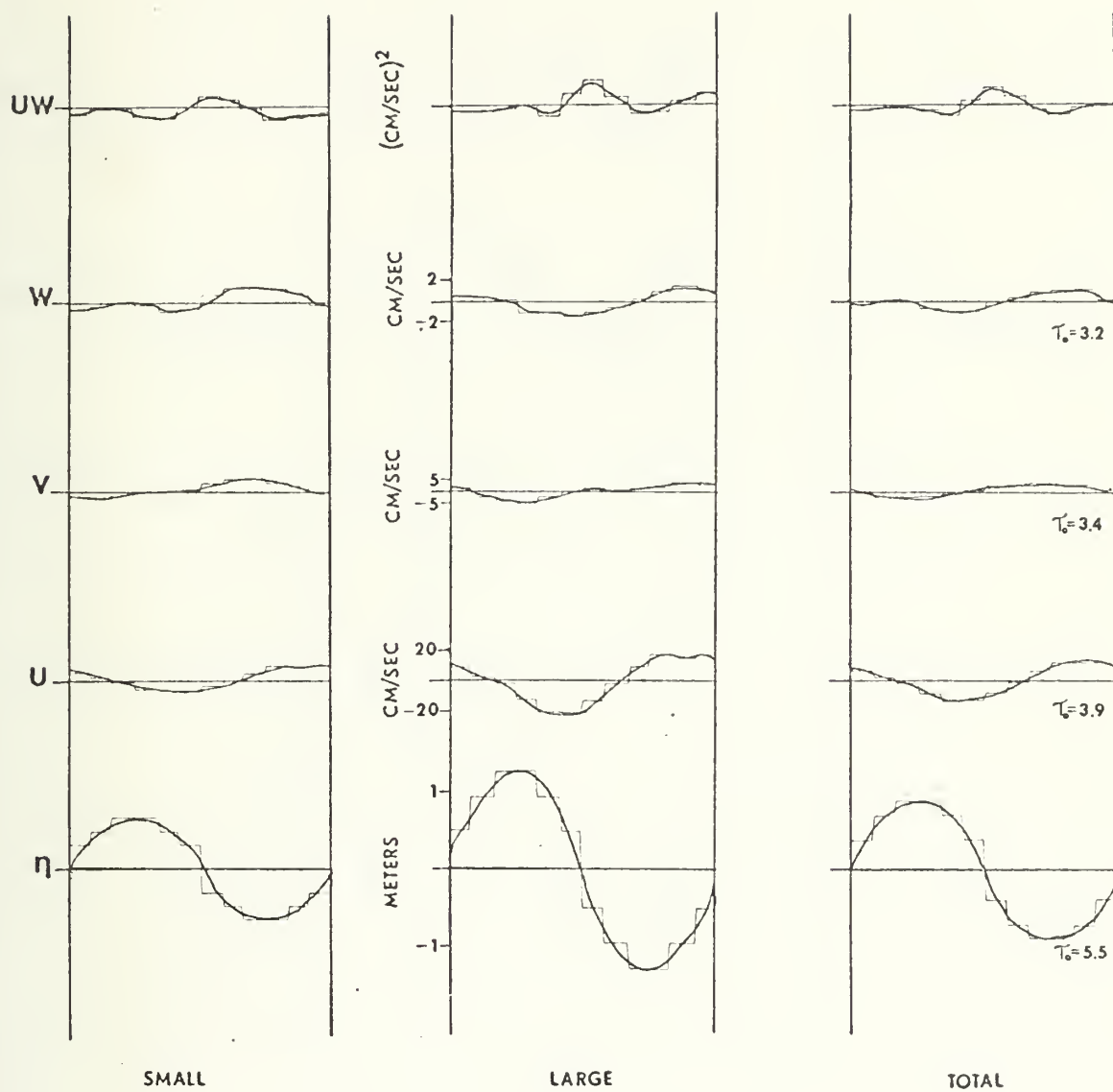


Figure 19. Phase-Amplitude Results for Period 1, Subset 3.

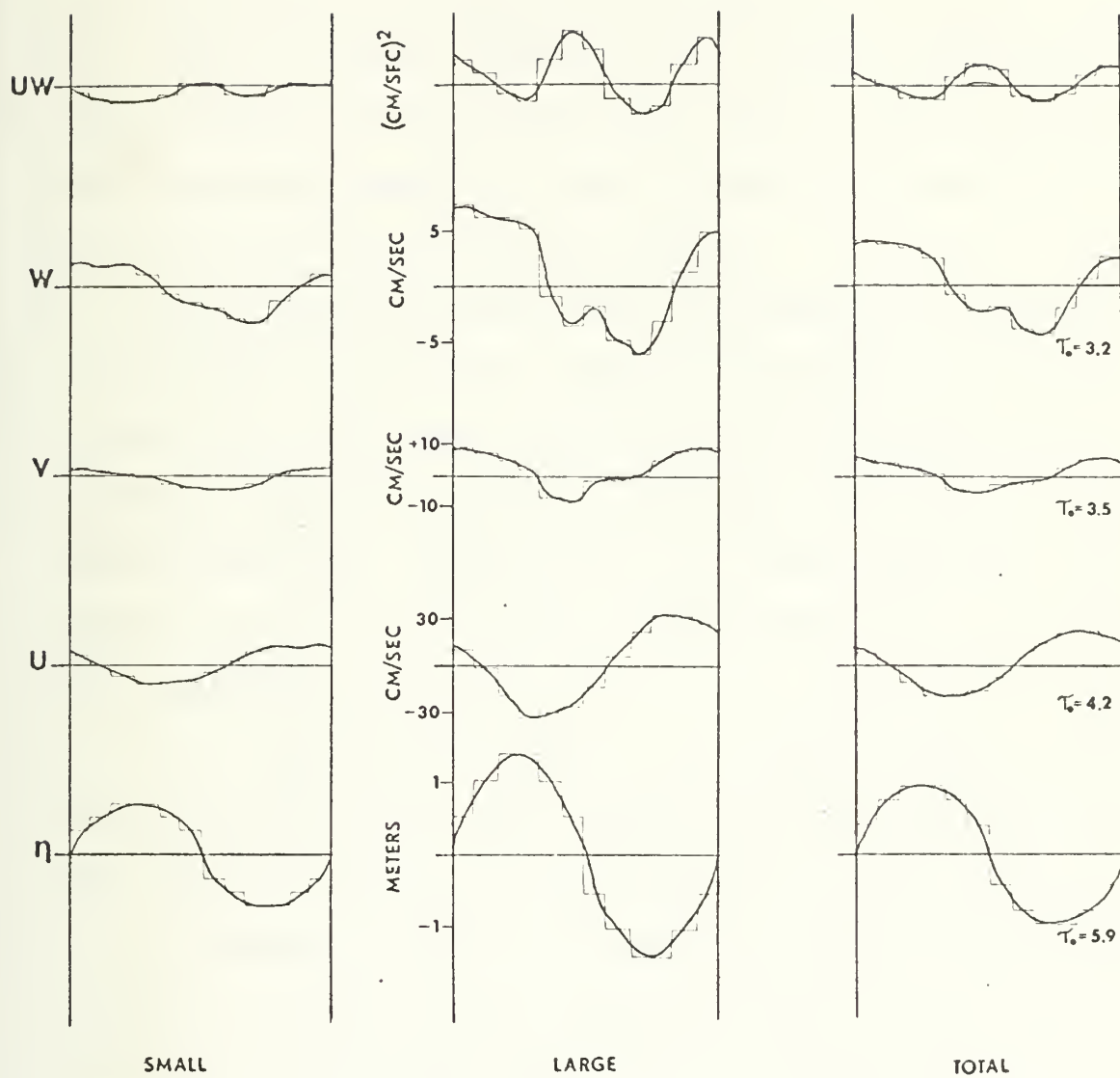


Figure 20. Phase-Amplitude Results for Period 1, Subset 4.

C. PERIOD 6

Measurements in period 6 were made at 8 meters and it is characterized by the low mean wind speed of 7.0 M/sec and the lowest observed wave heights at three to five feet. Wave heights had been diminishing during the previous six hours and wind speeds had been increasing slightly up to the time of the period, then diminishing.

The significant feature of this period, as indicated in Figures 21, 22, and 23 is that of all periods examined it seems to be very nearly as predicted by potential flow theory. This is especially discernable for the total waves phase-amplitude. However, there are some departures from potential flow in the phase relationships of u and w and in the amplitudes of uw .

The slight shift forward of the negative extrema of the w fluctuations will also be noted in period 14 and will be described in detail in the discussion of that period.

In subset 1 (Figure 21) there is a shift forward in the negative extrema of the u component while the positive extrema is consistent with results of period 12. The positive/negative extrema in u for the remainder of the period are also consistent with previous discussions in period 12 at the 8 meter level.

Potential flow theory predicts equal magnitudes (Figure 1) of uw in all quadrants. In these results the amplitudes vary over the phase of the wave and from subset 1 to subset 3.

In subset 1, Figure 21, quadrant IV, the amplitude values are greater than the other quadrants as evidenced by the predominance of the downward transfer of excess momentum. By the end of the period the dominant quadrant is quadrant II, indicative of an upward transfer of deficit momentum. In the total wave, however, quadrant II dominates in subsets 1 and 2, shifting to quadrant IV in subset 3. The total wave now closely resembles that predicted by potential flow theory.

No determinations concerning FLIP's motion seem possible from this period; however, with the small observed wave heights and a minimum of wind it is considered that the errors introduced were minimal.

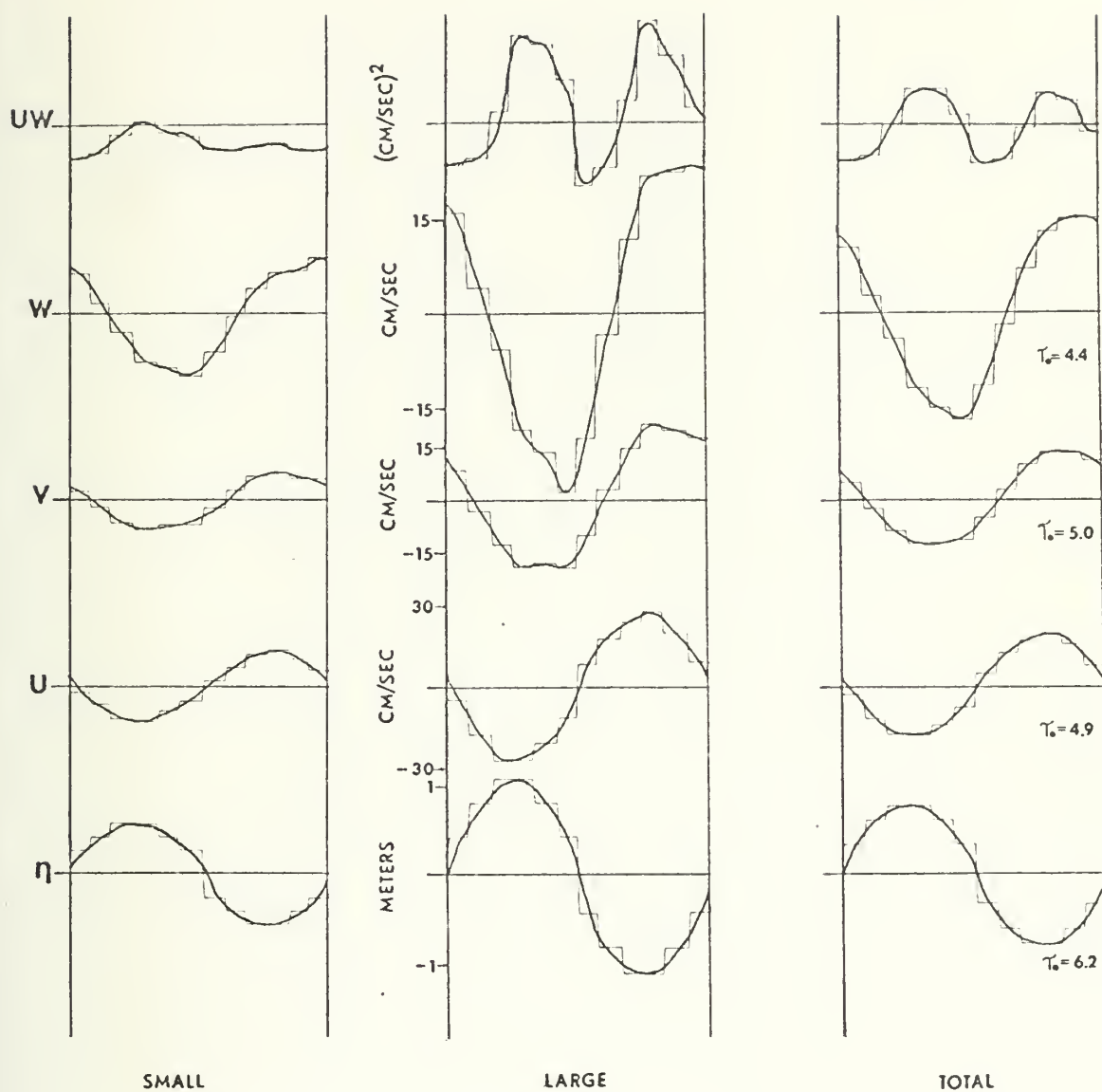


Figure 21. Phase-Amplitude Results for Period 6, Subset 1.

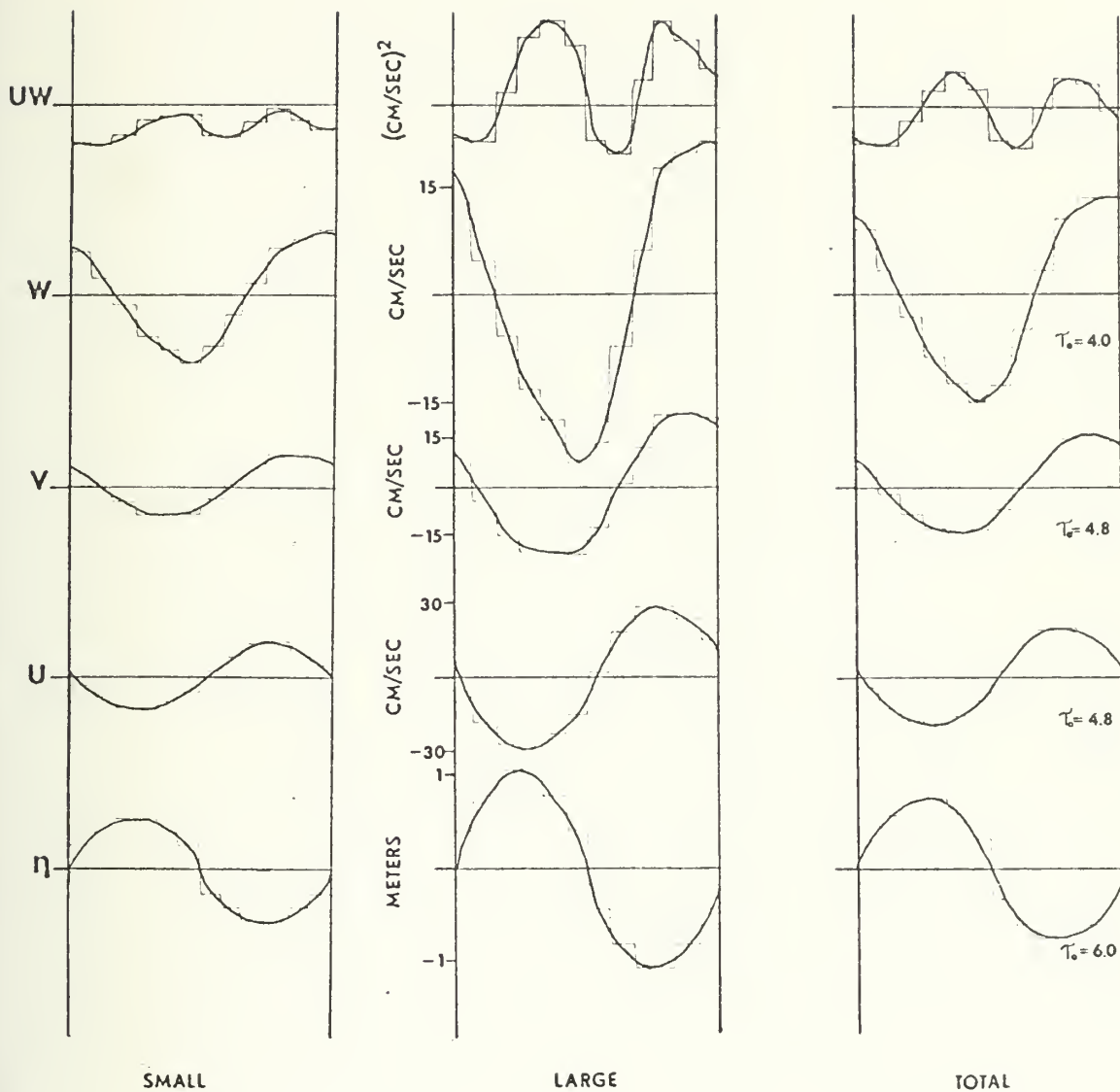


Figure 22. Phase-Amplitude Results for Period 6, Subset 2.

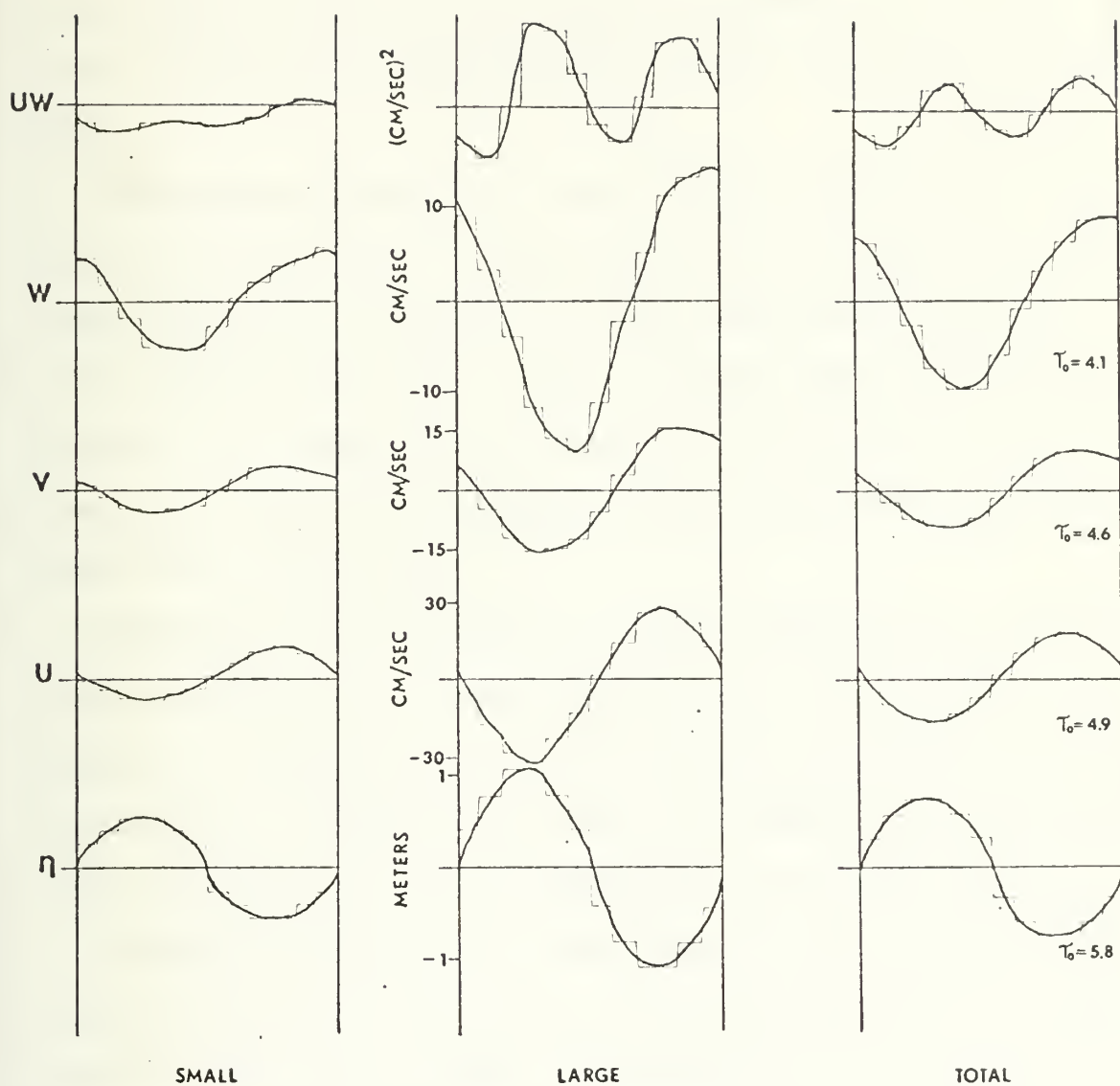


Figure 23. Phase-Amplitude Results for Period 6, Subset 3.

D. PERIOD 14

This period is unique in that measurements were made at the 3 meter level and thus offers a comparison with the lower level of period 12 and Thompson's (1972) results of the same data.

Significant features include distinct deviations from potential flow theory in the phase of w and the phase and amplitude of uw . Features of this period also deviate considerably from those for the 3 meter level in period 12. However, in comparison to period 12, this period's mean wind speed was only 7.6 M/sec and the observed wave heights were only six to eight feet.

The phase relationships of u are comparable to potential flow in subsets 1, 2, and 3 (Figures 24, 25, and 26), except for the consistent shift to the back node of the crest of the wave. However, in Figure 27, subset 4, it can be seen that the shift of u is to the front side of the crest.

Thompson had noted the occurrence in this period of a minimum value of w before the inflection point of the wave. However, with the increase in resolution, this shift is considered minor and should a further increase in resolution be achieved it is doubtful that the shift would be discernible at all. There is a considerable shift forward of the positive extreme of w which is a distinct departure from potential flow predictions where the maximum w values should occur at the inflection point of the wave at the end of

quadrant IV. The shift observed in this period varies from 30° to 90° forward and accounts for the predominance of the downward transfer of excess momentum in quadrant IV.

The discussion by Thompson (1972) of the uw phase-amplitude results is consistent with these results from the same data and will not be repeated here.

The differences between this period and the 3 meter level of period 12 seem to be the result of the reduced wind speeds and wave heights. In the u component there is no difference between the phase relationships of the two periods. The amplitude of the u component fluctuations is greater in the period with the lower mean wind speeds and wave heights, which may also explain the differences in the phase of w between the two periods. It does not seem likely that FLIP's motion would have led to these differences. The results in period 12 are considered to be consistent with measurements from a fixed platform by Davidson and Frank (1973) which were also in agreement with recent turbulence models. If Pond's (1967) suggestion concerning the tilt of the sensor platform is considered, the reduced tilt associated with reduced wave heights would certainly not lead to increases in the oscillations of FLIP and introduce an increased error. These differences in the results must then be attributed to a changing significance for the role of turbulence at various combinations of wind speed and wave height.

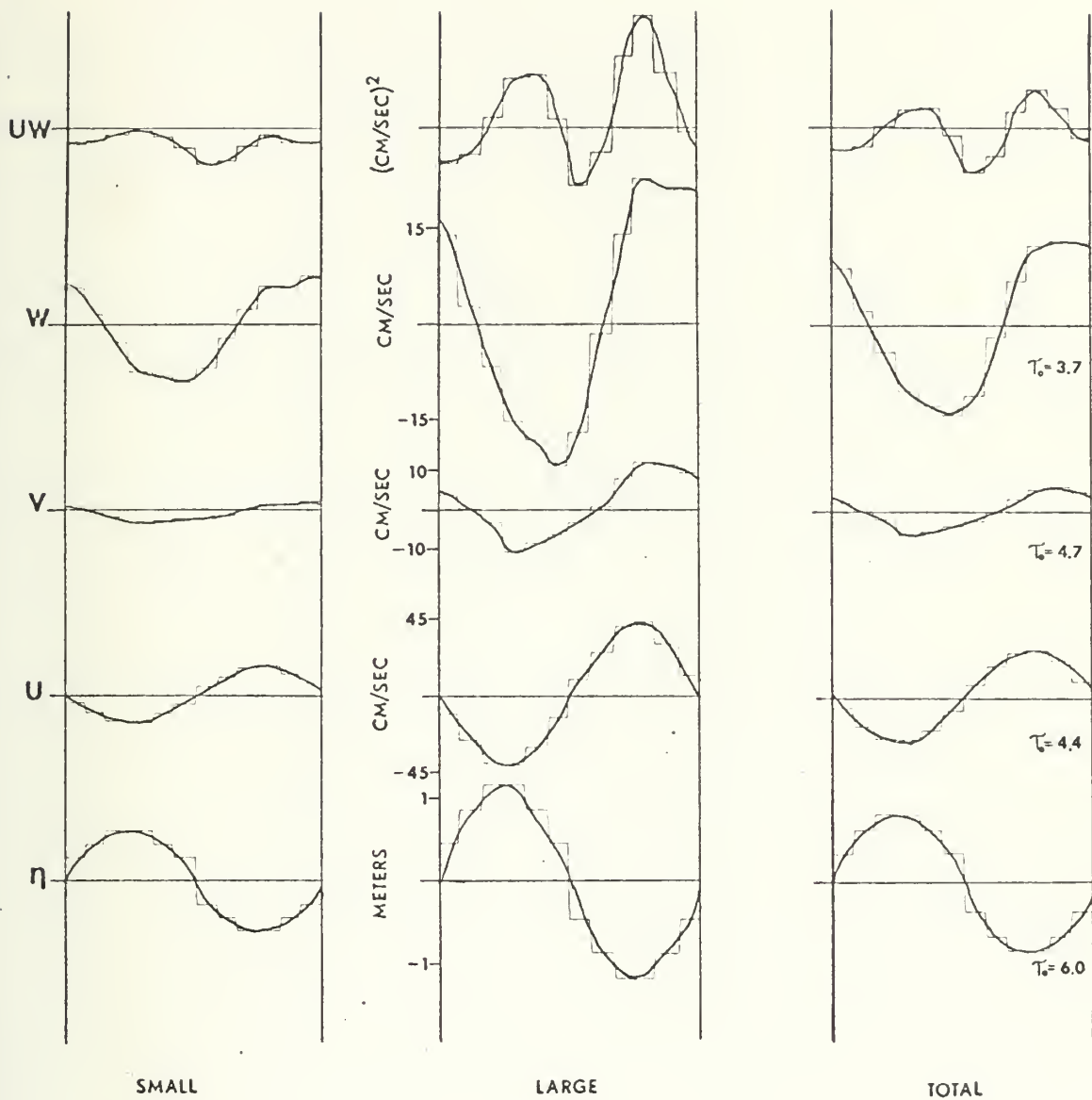


Figure 24. Phase-Amplitude Results for Period 14, Subset 1.

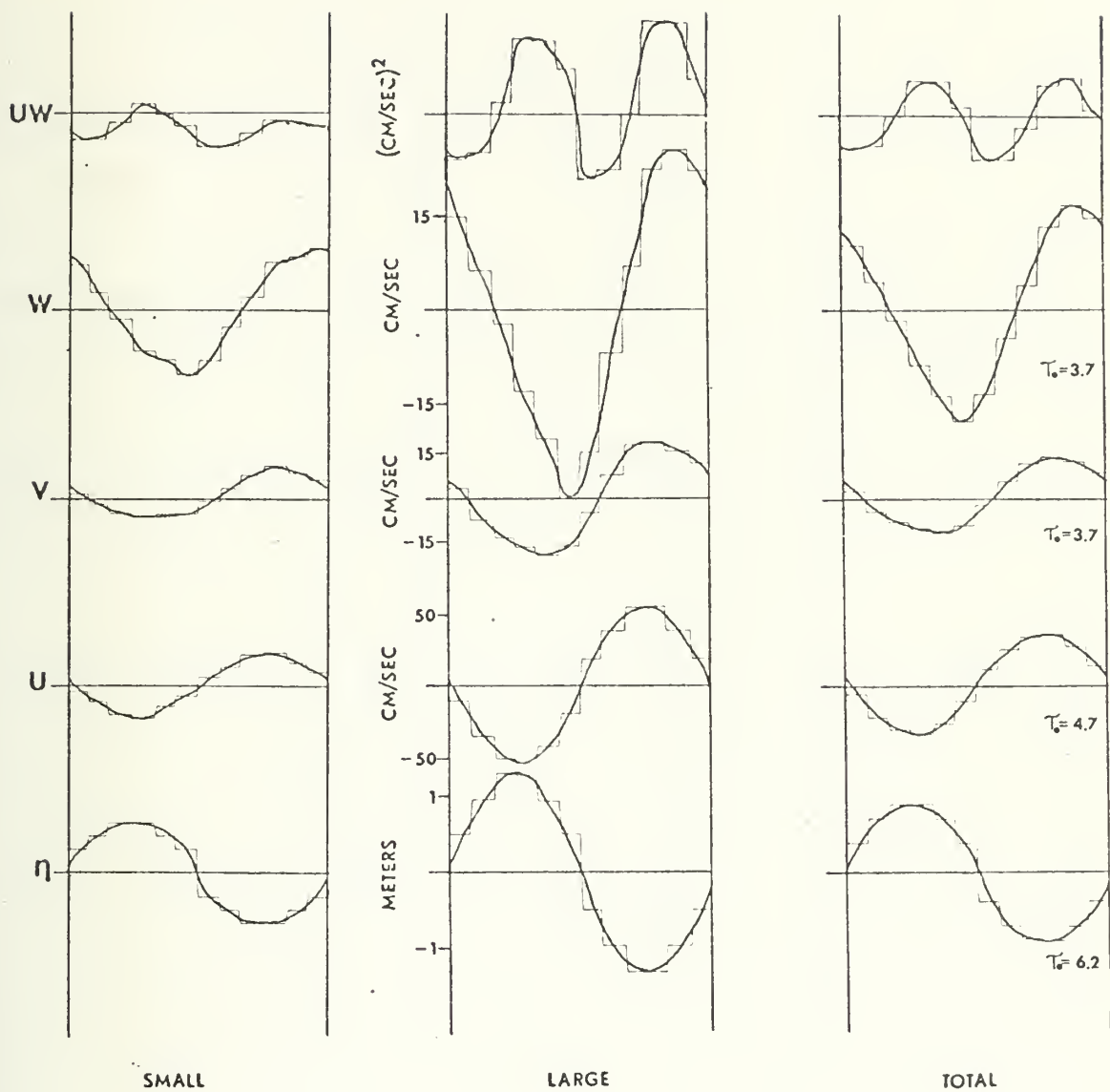


Figure 25. Phase-Amplitude Results for Period 14, Subset 2.

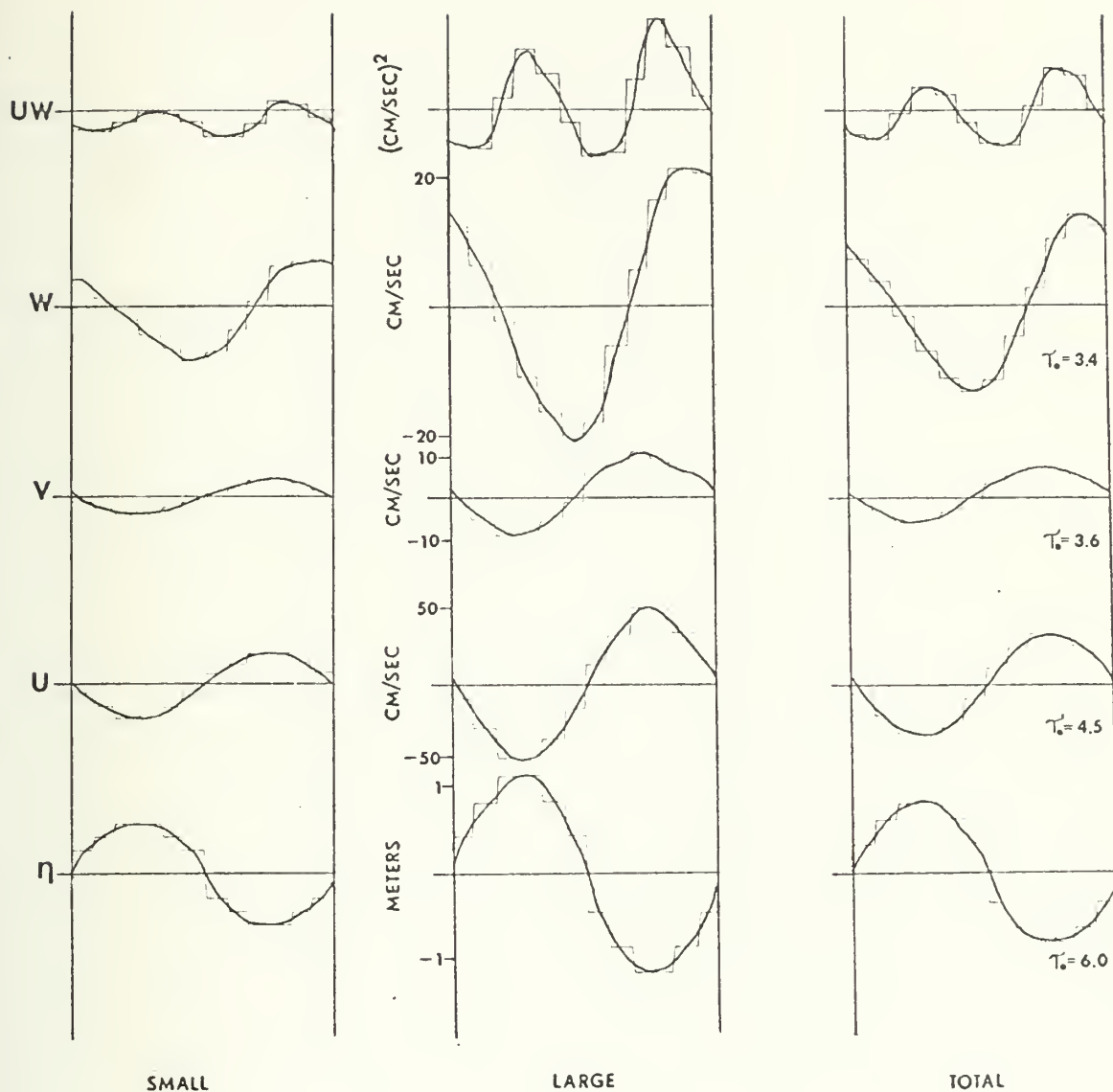


Figure 26. Phase-Amplitude Results for Period 14, Subset 3.

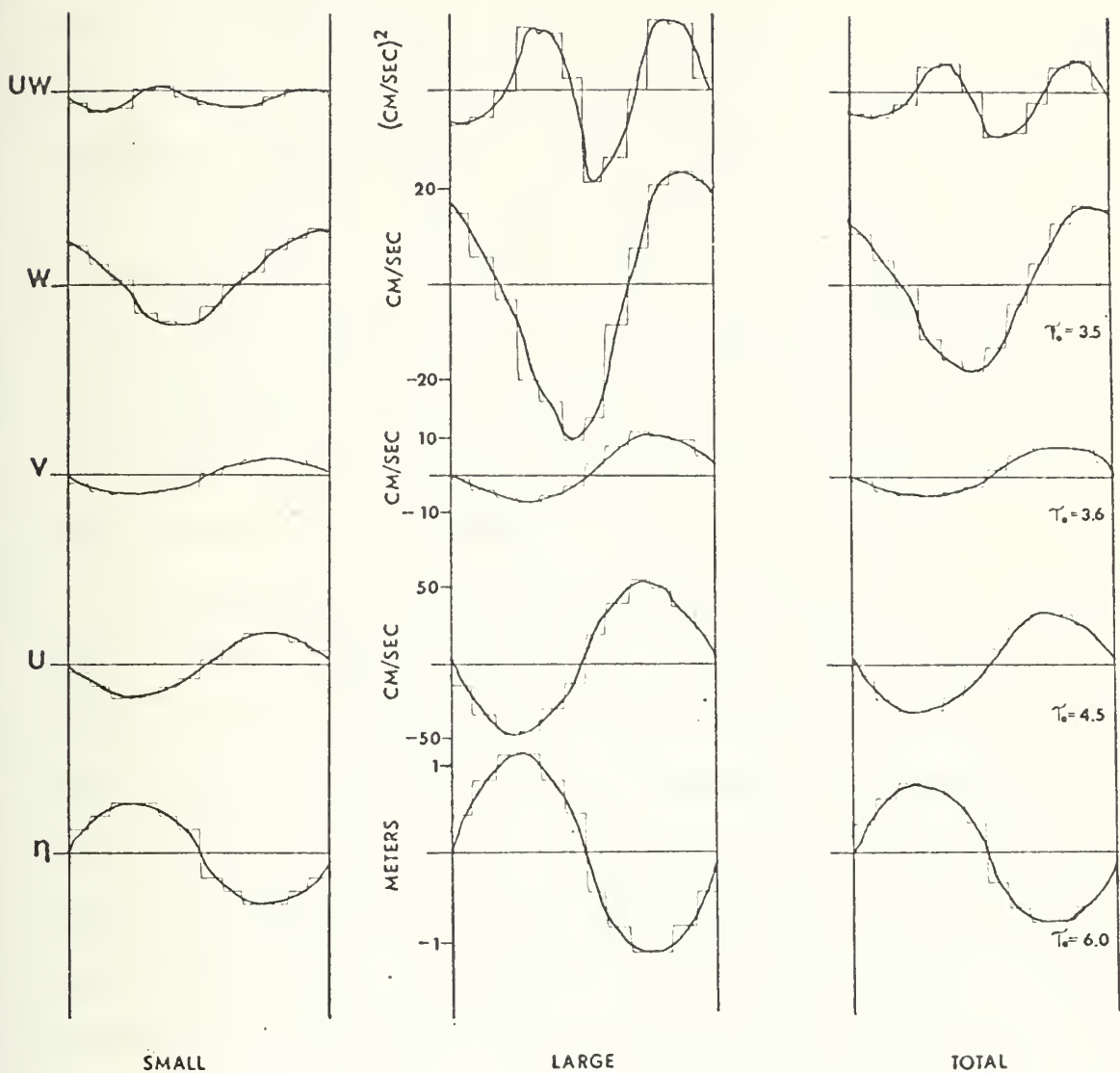


Figure 27. Phase-Amplitude Results for Period 14, Subset 4.

VI. SUMMARY AND CONCLUSIONS

Analyses were performed on observational data obtained over ocean waves from a relatively stable floating platform. The analyses on these data provided results on the phase and amplitude relationships of wave-related velocity fluctuations and wave heights. The results were interpreted with respect to potential flow predictions for a wave propagating beneath a shear flow and the role of turbulence in wind-wave coupling. Interpretations were also made with respect to the possible influence FLIP may have had on the data and the results of the analysis of that data.

A significant feature was the consistent phase relationship of the velocity component u , with that of the wave. In almost all cases there was a shift of 15° to 30° of the negative/positive extrema of the u component to the upwind side of the wave crest/trough. Although this feature is very similar to that predicted by potential flow theory, it is considered to be a significant deviation from the 180° phase difference predicted. Also observed was the absence of the quadrature relationship of u and w as predicted by potential flow. Deviations from potential flow predictions were interpreted to be indicative of interaction between the wave-induced motion and the shear flow. Thus a provision for turbulence interaction should be considered essential to wind-wave coupling models.

In comparison to potential flow predictions which have equal magnitudes of uw in all quadrants, the uw phase-amplitude

results revealed variations in magnitude over different phases of the wave. This suggests that nonlinear processes are responsible for momentum transfer in wind-wave coupling.

From comparisons with similar results from a fixed sensor platform and an examination of the phase relationships in the present results, it was concluded that the floating instrument platform had no appreciable effect on these results. However, results from similar investigations with real time measurements of platform motion are needed to strengthen this conclusion.

APPENDIX A¹

FLIP's motion will be described relative to a fixed reference coordinate system which has its origin at the equilibrium point of the buoy's metacenter (Figure 28). The terms pitch, roll, and yaw are the angular displacements (rotations) about the x, y, and z axes, respectively. Heave motion refers to displacements in the vertical (z) plane. Using these definitions the velocity of any point on the buoy can be found relative to the fixed system,

$$(1) \quad \vec{U}_R = \vec{U}' + \vec{\omega} \times \vec{r} ,$$

where U_R is the resultant vector velocity of a point on the buoy due to the linear velocity, \vec{U}' , of the buoy with respect to the fixed origin, and $\vec{\omega} \times \vec{r}$ (Figure 28) is the tangential velocity of the point about this origin. Measurements are taken with respect to the moving system, so the apparent velocity relative to the moving point on the buoy is

$$(2) \quad \vec{U}' = \vec{U}_R - \vec{\omega} \times \vec{r} .$$

This is the velocity detected by the anemometer on board FLIP, if there is no wind. If a "real" wind (U_w) field

¹Appendix A is unpublished work by Dr. A. W. Green, Department of Meteorology and Oceanography, University of Michigan. It has been revised slightly for inclusion in this thesis.

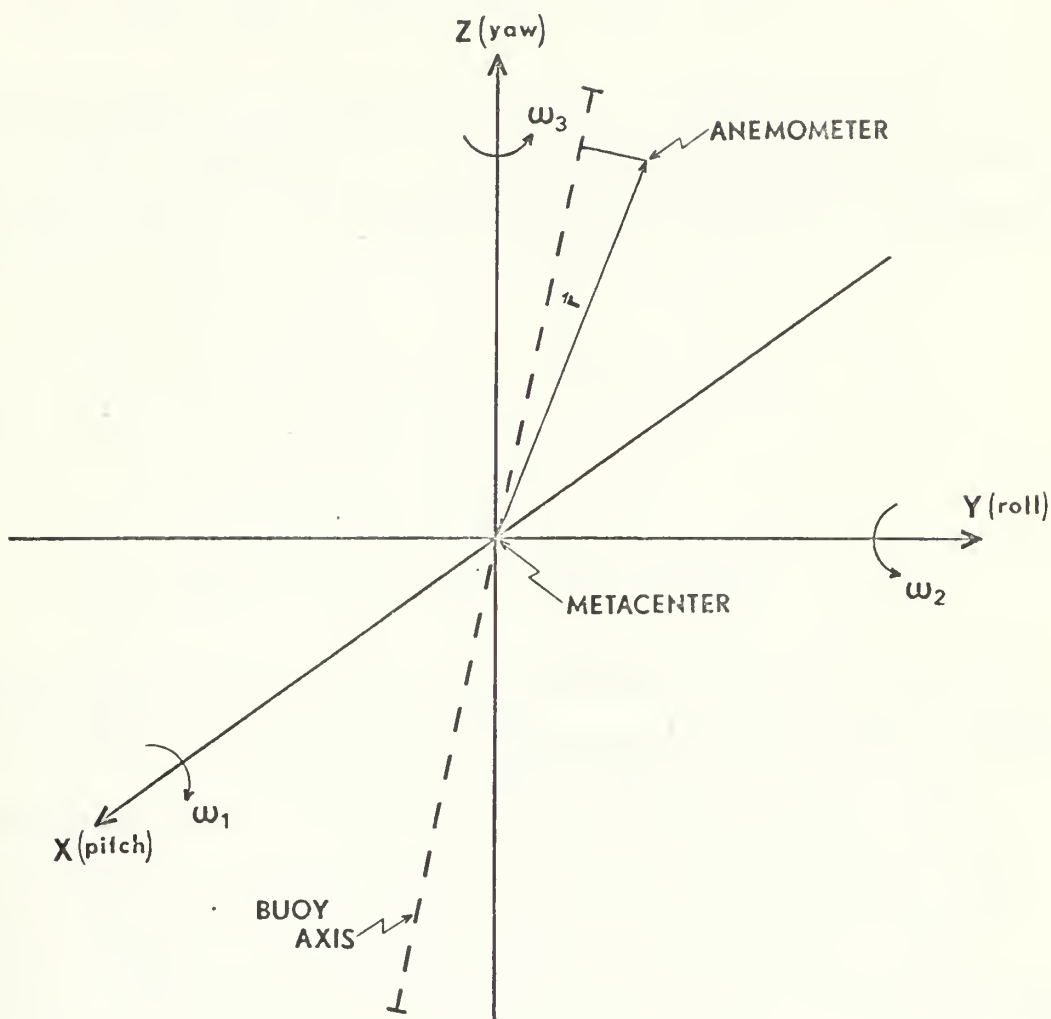


Figure 28. The fixed reference coordinate system has its origin at the metacenter of the spar buoy. For small pitch-roll displacements the metacenter is fixed. (See H. Lamb's Statics, p. 225, Cambridge Press, 1960.)

moving past the buoy is added, and only apparent velocities due to the heave ($\vec{U}_h = \hat{k}w_h$) plus rotation about the meta-center are considered, then (2) may be rewritten as

$$(2a) \quad \vec{U}' = \vec{U}_w + \vec{U}_h - \vec{\omega} \times \vec{r} = \vec{U}_w + \hat{k}w_h - \vec{\omega} \times \vec{r},$$

where w_h is the oscillation along the vertical due to heave sensed by the anemometers. \vec{U}_w is equal to the instantaneous "real" wind vector. Now equation (2) is placed in component form.

$$(a) \quad u' = u_w - (\omega_2 z - \omega_3 y)$$

$$(3) \quad (b) \quad v' = v_w - (\omega_3 x - \omega_1 z)$$

$$(c) \quad w' = w_w + w_h - (\omega_1 y - \omega_2 x)$$

The quantities $\omega_1, \omega_2, \omega_3$ can be defined as the roll, pitch, and yaw rates; x, y, z are the instantaneous distances along the respective axes for the equilibrium metacenter. The drift of FLIP due to the currents and wind will be ignored, although it could be important in cases of very low wind velocities. Next consider some of the statistical properties of the apparent wind field.

The power spectral density is usually computed from the auto-correlation of a time series of the velocity fluctuations, which may be represented by

$$(4) \quad Ru'(\tau) = \lim_{T \rightarrow \infty} \frac{1}{T} \int_{-T/2}^{T/2} u'(t) u'(t+\tau) dt$$

where $R_{u'}(\tau)$ is the auto-correlation function of the apparent x-component of the measured wind field with the time lag, τ . The power spectral density is

$$(5) \quad G_{u'}(f) = 2 \int_{-\infty}^{\infty} R_{u'}(\tau) e^{-i2\pi f\tau} d\tau$$

Coherent sinusoidal motions will then give peaks in the power spectral density plots. Taking two examples, the effects of buoy motion on the power spectrum will be shown.

1. The auto-correlation function of the horizontal fluctuation component at zero lag ($\tau = 0$), (the bar indicates time average).

$$(6) \quad R_{u'}(\tau=0) = \overline{u'u'} = \overline{u_w u_w - 2u_w(\omega_2 z - \omega_3 y) + (\omega_2 z - \omega_3 y)^2}$$

(1)
(2)
(3)

2. The cross correlation function of the horizontal and vertical fluctuations, or Reynolds' stress,

$$(7) \quad \overline{u'w'} = \overline{U_w w_w + u_w w_h - u_w(\omega_1 y - \omega_2 s) - w_w(\omega_2 z - \omega_3 y)}$$

(1)
(2)
(3)
(4)

$$\overline{-w_h(\omega_1 y - \omega_2 x) + (\omega_2 z - \omega_3 y) \cdot (\omega_1 y - \omega_2 x)}$$

(5)
(6)

The first term on the r.h.s. of (6) is the mean square fluctuation, or the "true zero-lag." The second is the correlation of the wind fluctuation with the pitch and yaw

motions, which could have the effect of decreasing the apparent mean square values. Finally the last term represents the apparent net mean square of the correlated motion of pitch and yaw, which must be positive. It should be noted that the yaw and pitch velocities are the total instantaneous motions due to the rotation of the sensor probe about the reference axes. Consequently, the terms buoy motion represents are the instantaneous apparent velocity components which by themselves have a virtually continuous spectrum. According to Rudnick's (1967) measurements of FLIP's motion, the spectra tend to have peaks which roughly correspond to the wave frequency, pitch-roll, and heave resonances. Also the nonlinear response of the buoy can lead to higher order responses which would give peaks in power at several combination frequencies of the above.

The first term on the r.h.s. of (7) is the "real" Reynolds stress. The second term could be troublesome since its absolute magnitude could be large, if there is a wind component which correlates significantly with the vertical velocity due to heave. The third term is the correlation of the wind fluctuations and the vertical velocities due to pitch and roll. The fourth is the correlation of the vertical wind fluctuation and the pitch and yaw motions. The fifth term is the correlation of yaw-pitch with roll-pitch motions of the buoy; this term is probably negative since the pitch-pitch correlation, $(\omega_2 z) \cdot (-\omega_2 x)$ is less than zero. BOMEX

data motion spectra have relatively sharp peaks at lower frequencies with lower values for $u'w'$ than other observers. A probable reason is the presence of the fourth and fifth terms of (7) which may have negative values that tend to decrease the mean Reynolds stress.

Apparent FLIP motions, which are more or less sinusoidal, may be conveniently represented as the super-positions of the components of the apparent velocity in the following way,

$$\begin{aligned}
 (8)^1 \quad \vec{\omega} \times \vec{r} + \hat{k}w_h = \sum_n \{ (\hat{i}\omega_{1,n} + \hat{j}\omega_{2,n} + \hat{k}\omega_{3,n}) \times [\hat{i}x_n \cos(\omega_{1,nt}) \\
 + \hat{j}y_n \sin(\omega_{2,nt} + \phi_n) + kz_n \sin(\omega_{3,nt} + \phi'_n) \\
 + \hat{k}\omega_{h,n} z_h \sin(\omega_{h,nt} + \phi_{h,n})] \}
 \end{aligned}$$

where summation is over all modes of FLIP.

¹ $\phi_n, \phi'_n, \phi_{h,n}$ are random phase variations; x_n, y_n, z_n, z_h are the maximum displacements from equilibrium position associated with a given mode.

BIBLIOGRAPHY

1. Bingham, G. S., Spectra of Turbulent Fluctuations over Ocean Waves, M.S. Thesis, Naval Postgraduate School, Monterey, California, 1972.
2. Bronson, E. D., and Glasten, L. R., FLIP, Floating Instrument Platform, SIO Reference 65-12, ONR Contract Nonr 2216 (05), Scripps Institution of Oceanography, San Diego, Cal. 21 p., 1968.
3. Davidson, K. L., An Investigation of the Influence of Water Waves on the Adjacent Airflow, ORA Report 08849-2-T, ONR Contract N0014-67-A-0181-005, Department of Meteorology and Oceanography, University of Michigan, 259 pp., 1970.
4. Davidson, K. L., and Frank, A. J., "Properties of Wave-Related Fluctuations in the Airflow above Natural Waves," Journal of Physical Oceanography, 3(1), p. 102-119, 1973.
5. Davis, R. E., "On Prediction of the Turbulent Flow over a Wavy Boundary," Journal of Fluid Mechanics, 52, p. 721-732, 1972.
6. Holland, J. Z., "A Statistical Method for Analyzing Wind Shapes and Phase Relationships of Fluctuating Geophysical Variables," Journal of Physical Oceanography, 3(1), p. 139-155, 1973.
7. Kendall, J. M., "The Turbulent Boundary Layer over a Wall with Progressive Surface Waves," Journal of Fluid Mechanics, 41(2), p. 259-281, 1970.
8. Kondo, J., Fujinawa, V., and Naito, G., "Wave-Induced Wind Fluctuations over the Sea," Journal of Fluid Mechanics, 51, p. 751-771, 1972.
9. Miles, J. W., "On the Generation of Surface Waves by Shear Flows," Journal of Fluid Mechanics, 3(2), p. 185-204, 1957.
10. Möllo-Christensen, E., Wind Tunnel Test of the Superstructure of R/V FLIP for Assessment of Wind Field Distortion, Rept. No. 68-2, Fluid Dynamics Laboratory, Massachusetts Institute of Technology, 1968.
11. Pond, S., "Some Effects of Buoy Motion on Measurements of Wind Speed and Stress," Journal of Geophysical Research, 73(2), p. 507-512, 1968.

12. Pond, S., Phelps, G. T. and Paquin, J. E., "Measurements of the Turbulent Fluxes of Momentum, Moisture and Sensible Heat over the Ocean," Journal of Atmospheric Sciences, 28(6), 1971.
13. Portman, D. J., Davidson, K. L., and Walter, M. A., An Investigation of the Structure of Turbulence and of the Turbulent Fluxes of Momentum and Heat over Waves, ORA Report 08849-3-P, ONR Contract N0014, 67-A-0181-005, Department of Meteorology and Oceanography, University of Michigan, 40 pp., 1970.
14. Reynolds, W. C., The Mechanics of an Organized Wave in a Turbulent Shear Flow, unpublished manuscript, Department of Mechanical Engineering, Stanford University, 39 pp., 1968.
15. Rudnick, P., "Motion of a Large Spar Buoy in Sea Waves," Journal of Ship Research, 11(4), p. 257-267, 1967.
16. Stauffer, B. S., Application of a Theoretical Model to Velocity Fields Observed over Water Waves, M.S. Thesis, Naval Postgraduate School, Monterey, California, 1973.
17. Superior, W. J., BOMEX Flux and Profile Measurements from FLIP, Final Report, Naval Oceanographic Office Contract N62306-69-C-0186, C. W. Thornthwaite Associates, Laboratory of Climatology, Elmer, N.J., 32 pp., 1969.
18. Thompson, S. P., Wave-Related Disturbances in the Velocity Field over Ocean Waves, M.S. Thesis, Naval Postgraduate School, Monterey, California, 1972.
19. Yefimov, V. V., "On the Structure of the Wind Velocity Field in the Atmospheric Near-Water Layer and the Transfer of Wind Energy to Sea Waves," Atmospheric and Oceanic Physics, 6(19), p. 1043-1058, translated by McIntosh, J. D. L., 1970.

INITIAL DISTRIBUTION LIST

	No. Copies
1. Defense Documentation Center Cameron Station Alexandria, Virginia 22314	2
2. Library, Code 0212 Naval Postgraduate School Monterey, California 93940	2
3. Professor Kenneth L. Davidson, Code 51 Ds Department of Meteorology Naval Postgraduate School Monterey, California 93940	10
4. Department of Meteorology Naval Postgraduate School Monterey, California 93940	2
5. Professor G. J. Haltiner, Code 51 Ha Department of Meteorology Naval Postgraduate School Monterey, California 93940	1
6. Commander, Naval Weather Service Command Naval Weather Service Headquarters Washington Navy Yard Washington, D. C. 20390	1
7. Dr. Donald J. Portman Department of Meteorology and Oceanography University of Michigan Ann Arbor, Michigan 48103	1
8. Professor R. T. Williams, Code 51 Wu Department of Meteorology Naval Postgraduate School Monterey, California 93940	1
9. Professor R. L. Haney, Code 51 Hy Department of Meteorology Naval Postgraduate School Monterey, California 93940	1
10. Lieutenant David R. Aurand, USN 42 Townhouse Lane Corpus Christi, Texas 78412	3

UNCLASSIFIED

Security Classification

DOCUMENT CONTROL DATA - R & D

(Security classification of title, body of abstract and indexing annotation must be entered when the overall report is classified)

ORIGINATING ACTIVITY (Corporate author)

Naval Postgraduate School
Monterey, California 93940

2a. REPORT SECURITY CLASSIFICATION

Unclassified

2b. GROUP

REPORT TITLE

Wave-Related Velocity Fluctuations over Ocean Waves as Measured
from FLIP during BOMEX

DESCRIPTIVE NOTES (Type of report and, inclusive dates)

Master's Thesis; March 1973

AUTHOR(S) (First name, middle initial, last name)

David Robert Aurand

REPORT DATE

March 1973

7a. TOTAL NO. OF PAGES

71

7b. NO. OF REFS

19

CONTRACT OR GRANT NO.

9a. ORIGINATOR'S REPORT NUMBER(S)

PROJECT NO.

9b. OTHER REPORT NO(S) (Any other numbers that may be assigned
this report)

DISTRIBUTION STATEMENT

Approved for public release; distribution unlimited.

SUPPLEMENTARY NOTES

12. SPONSORING MILITARY ACTIVITY

Naval Postgraduate School
Monterey, California 93940

ABSTRACT

Wave-related velocity fluctuations over ocean waves and wave heights as measured from FLIP during BOMEX are examined using phase-amplitude results which are based on joint probability density function-conditional mean function (JPDF-CMF) analyses. Results are compared with predictions from various wind-wave coupling models.

Results are examined in detail and consistent departures from theory are noted. An attempt is made to qualitatively determine the effect on specific results of the moving, but relatively stable, sensor platform, FLIP.

It is concluded that the interaction between the wave-induced motion and airflow turbulence had a significant effect on the observed wave-related fluctuations. The effects of FLIP on the results appeared to be minimal on these results.

UNCLASSIFIED

Security Classification

KEY WORDS	LINK A		LINK B		LINK C	
	ROLE	WT	ROLE	WT	ROLE	WT
Turbulence						
Floating Instrument Platform						
Wave-induced Motion						
Observational Data						
Potential Flow Predictions						
Wind-wave Coupling						

Thesis

A963 Aurand

c.1

Wave-related velocity
fluctuations over ocean
waves as measured from
FLIP during BOMEX.

143268

Thesis

A963 Aurand

c.1

Wave-related velocity
fluctuations over ocean
waves as measured from
FLIP during BOMEX.

143268

thesA963

Wave-related velocity fluctuations over



3 2768 001 91066 4

DUDLEY KNOX LIBRARY